1972

Thin film Pb(0.9)Sn(0.1)Se photoconductive infrared detectors, metallurgical and electrical measurements.

McBride, William Godfrey,Jr.

Monterey, California. Naval Postgraduate School

THIN FILM $Pb_{0.9}Sn_{0.1}Se$ PHOTOCONDUCTIVE INFRARED DETECTORS, METALLURIGICAL AND ELECTRICAL MEASUREMENTS

William Godfrey McBride

NAVAL POSTGRADUATE SCHOOL
Monterey, California

THESIS

THIN FILM $Pb_{0.9}Sn_{0.1}Se$ PHOTOCONDUCTIVE INFRARED DETECTORS, METALLURGICAL AND ELECTRICAL MEASUREMENTS

by

William Godfrey McBride, Jr.

Thesis Advisor: T. F. Tao

December 1972

Thin Film $Pb_{0.9}Sn_{0.1}Se$ Photoconductive Infrared Detectors, Metallurgical and Electrical Measurements

by

William Godfrey McBride, Jr.
Captain, United States Marine Corps
B.S., United States Naval Academy, 1966

Submitted in partial fulfillment of the
requirements for the degree of

MASTER OF SCIENCE IN ELECTRICAL ENGINEERING

from the

NAVAL POSTGRADUATE SCHOOL
December 1972

ABSTRACT

$Pb_{0.9}Sn_{0.1}Se$ thin films were deposited onto cleaved (111) CaF_2 and BaF_2 substrates by either an open one-boat evaporation method or a Knudson type graphite boat method. On CaF_2, single crystal (100), (111), and polycrystalline (100)+(111) films were obtained. On BaF_2, single crystal (111) and polycrystalline (111)+(100) films were achieved. As-deposited films were not photosensitive. Photoconductivity was observed after isothermal annealing in Pb/Sn rich vapor to reduce their carrier concentrations to the mid-10^{16} to mid-10^{17} range. (100) films were more sensitive than either single crystal (111) or polycrystalline (100)+(111) films. At 100°K, 500°K blackbody responsivities up to 60V/W have been developed, compared with the best blackbody responsivities around 100-125 V/W reported for commercial photovoltaic detectors of $Pb_{1-x}Sn_xTe$ operated at 77°K.

TABLE OF CONTENTS

LIST OF TABLES

Table

LIST OF FIGURES

Figure

ACKNOWLEDGMENTS

Appreciation is expressed to:

Doctor Tien Fan Tao for his inspiration and guidance

The United States Marine Corps for giving me the opportunity to obtain postgraduate education

and to the taxpayers of America in the hope that they will benefit from this and related research.

This thesis was made possible by the support of the Office of Naval Research and the Air Force Materials Laboratory.

I. INTRODUCTION

Considerable progress has been made in the past few years in developing long wavelength infrared (LWIR) devices for imaging, surveillance, remote sensing applications and for use in CO_2 laser systems. One of the most important advancements is the development of narrow gap IV-VI alloy semiconductor devices. Considerable attention has been given to two alloy systems, $Pb_{1-x}Sn_xTe$ and $Pb_{1-y}Sn_ySe$. Their p-n homojunctions now have adequate device performance when used as practical photovoltaic detectors (Ref. 1) and semiconductor lasers (Ref. 2). In comparison, photoconductivity in these two alloy systems has not been as well developed. Of these two alloys, $Pb_{1-x}Sn_xTe$ photoconductors have been relatively more developed than $Pb_{1-y}Sn_ySe$.

Photoconductivity in bulk $Pb_{1-x}Sn_xTe$ crystals was first studied at Lincoln Laboratory, MIT (Ref. 3). Subsequently, photoconductivity in $Pb_{1-x}Sn_xTe$ thin films were reported by Tao's group (Ref. 4) and Ford Scientific Laboratory (Ref. 5). The present $Pb_{1-x}Sn_xTe$ detector performances are presented in Table I. When operated at liquid nitrogen temperatures, peak responsivities (around 8-11 μ) are less than 10 V/W. Although several attempts have been made in developing $Pb_{1-y}Sn_ySe$ photoconductive detectors at RCA Princeton Research Laboratories, and General Electric Research Laboratories, no quantitative results indicating true photoconductivity in

TABLE I

PROPERTIES OF PHOTYCONDUCTIVE $Pb_{1-x}Sn_xTe$ BULK SINGLE CRYSTALS AND THIN FILMS

	Polycrystalline (100) films		Single crystal (111) film	Bulk (100) single crystals
	One boat evaporation	Flash evaporation		
Composition x	.20	0.14	0.17	.20
Thickness (u)	6.3	5	3	50
Sensitive area (cm^2)	0.2	0.21	0.25	0.015
Carrier concentration (cm^{-3})	2.8×10^{17} (p)	8×10^{16} (p)	3.9×10^{16} (n)	7.5×10^{15} (n)
Mobility ($cm^2V^{-1}sec^{-1}$)[a]	1×10^3	2×10^2	1.4×10^4	3.2×10^4
Temperature (°K)	100	77	77	77
Resistance (ohm)	250	9000	380	13
Bias (mA)	15	1.5	15	30
Peak wavelength (u)	9.6	8	8.9[b]	14
Peak responsivity (V/W)	4.8	9.7	13.2[c]	0.6
Peak detectivity ($cmW^{-1}Hz^{-½}$)	5.5×10^8	1.7×10^8	6.6×10^8	1×10^8

a. Electrical properties of (100) films measured at 87°K
b. Measured at 84°K
c. Multiply reported blackbody responsivity by 2.45

$Pb_{1-y}Sn_ySe$ has been reported. Some preliminary study of $Pb_{1-y}Sn_ySe$ photoconductive detectors has been done by Drs. I. Kasai and C. C. Wang.

The purpose of this thesis project was to develop more extensively $Pb_{1-y}Sn_ySe$ photoconductive detectors. The alloy composition y = 0.1 was selected because its energy gap at liquid nitrogen temperatures is suitable for infrared detection in the 8-14 micron atmospheric window. This was a joint thesis project by the author and LT.jg Kurt Holmquist, USN. Both of us were involved in all aspects of this research, although in the writing of the thesis, the author concentrated on the metallurgical and electrical properties and LT.jg Holmquist concentrated on the photoconductive properties.

II. PROPERTIES OF PB-SN-CHALCOGENIDE SEMICONDUCTOR ALLOYS

$Pb_{1-y}Sn_ySe$ is a member of the family of Pb-Sn-chalcogenide narrow-gap semiconductor alloys. Companion alloys include $Pd_{1-x}Sn_xTe$, $Pb_{1-w}Sn_wS$, and others. These alloys have been of recent interest because their energy-gaps can be made smaller than 0.4 ev which corresponds to photon energies in long wavelength infrared beyond three microns. A characteristic of these alloys which is of particular interest is the fact that their energy-gap can be made arbitrarily small by controlling the ratio of Sn-chalcogenide to Pb-chalcogenide and the temperature, a feature which has obvious advantages in tailoring the emission wavelength of their junction lasers and the photoresponse of their photodetectors.

A. MATERIAL PROPERTIES OF $Pb_{1-y}Sn_ySe$

Pb and Sn are members of the Group IV elements. When they are combined with the Group VI elements S, Se, and Te nine IV-VI compounds can be formed. Of these nine, PbSe and SnSe and studied in this report.

Some basic properties of PbSe and SnSe are shown in Table II. PbSe has a cubic rocksalt structure (B1), while SnSe has an orthorhombic (B29) structure (Ref. 6). Solid alloy mixtures of PbSe and SnSe can exist in either B1, B1 and B29, or B29 form, depending upon the relative proportion of each in the alloy and on the alloy temperature. These

TABLE II

SOME METALLURGICAL PROPERTIES OF IV-VI COMPOUNDS

Compound	Melting Point °C	Structure at 300°C	Energy-Gap at 300°C	Conductivity Type (undoped)
Sn Se	860	B29	.90	p
Pb Se	1081	B1	.29	n,p

This table is from Ref. 6

various conditions are shown in Figure 1 which is a temperature-composition diagram for PbSe-SnSe. It shows the phase of $Pb_{1-y}Sn_ySe$ as a function of T and y, and gives the structure of the resultant solidus alloys. For the y = .10 composition studied in this research, the melting point occurs at approximately 1030°C, and the system is completely liquid at 1070°C.

When stochiometric[1] quantities of PbSe and SnSe are melted at slightly above their melting point a pseudo-binary alloy of $Pb_{1-y}Sn_ySe$ is formed. Strauss (Ref. 7) has shown that for y less than .48 the resultant alloy has a rocksalt (B1) structure and a eutectic temperature of 870°C. If a temperature-composition diagram is constructed for a fixed value of y, and a variable PbSn to Se ratio p, a curve resembling that of Figure 2 is the result (Ref. 8). The

[1]Fifty percent metal, fifty percent chalcogenide (molar).

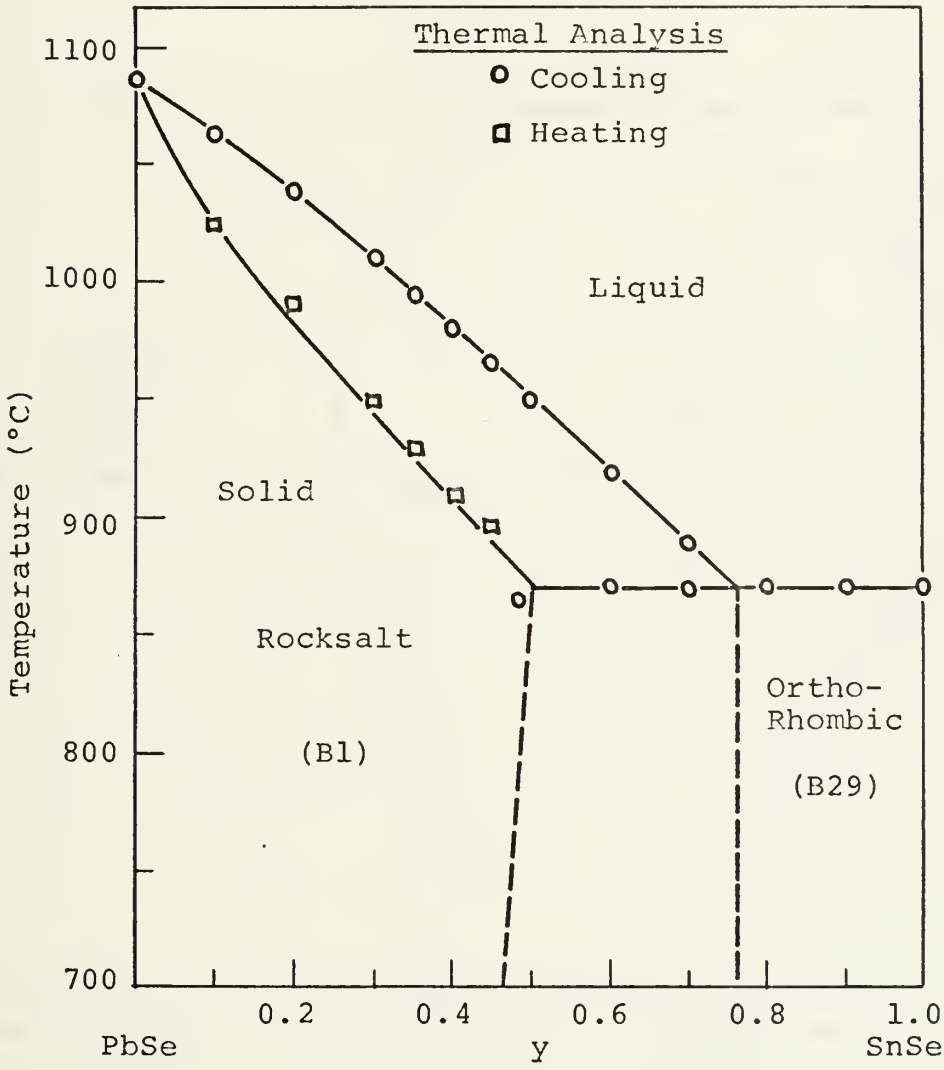

Figure 1. Temperature-Composition Diagram for $Pb_{1-y}Sn_ySe$ System.

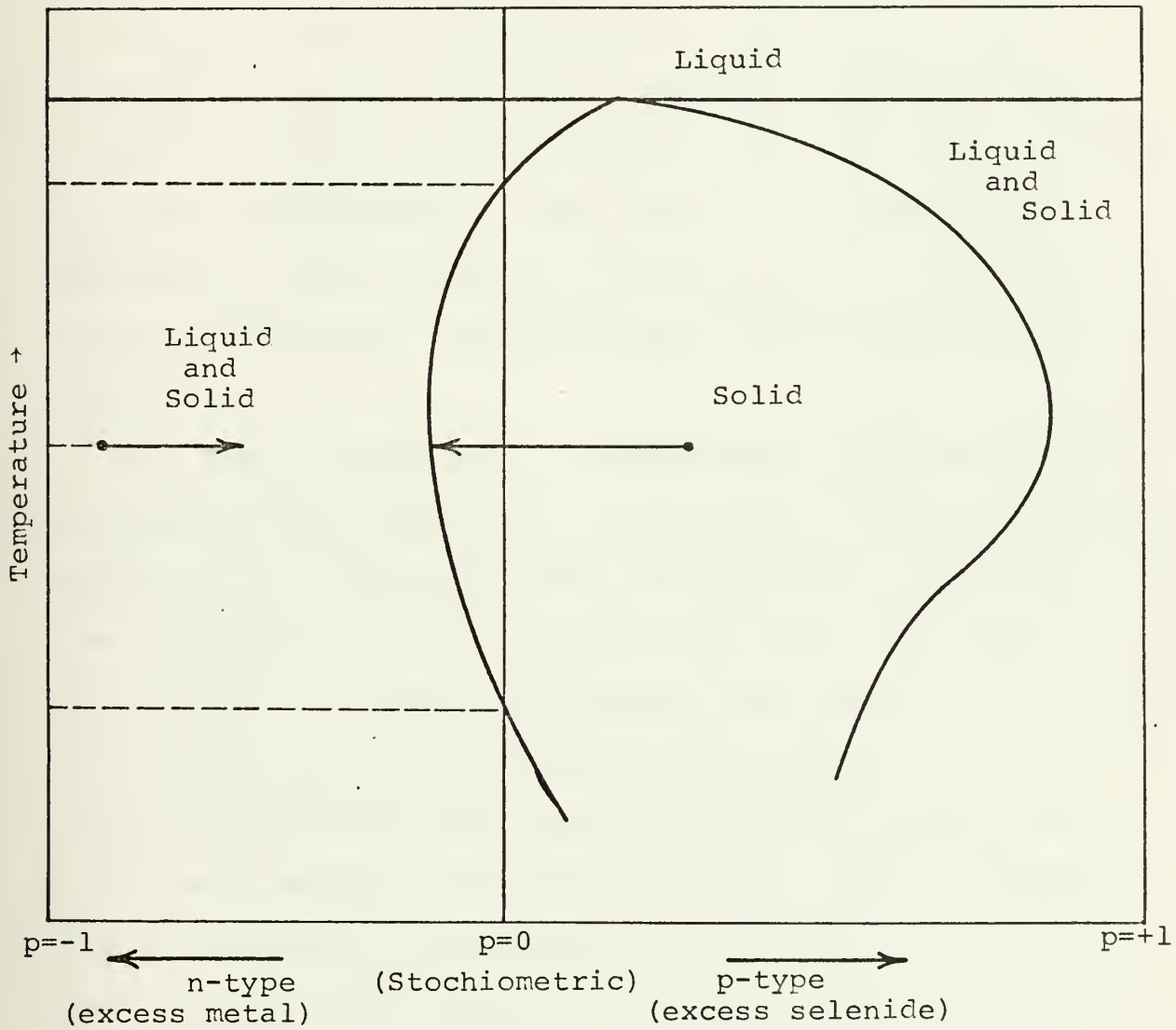

Figure 2. Temperature-Composition Diagram for a Fixed y, and a Variable Metal to Selenide Ratio, p for the Compound $(Pb_{1-y}Sn_y)_{0.5-p}(Se)_{0.5+p}$.

verticle dashed line at p = 0 is the stochiometric ratio. As p increases to the right of this line the mixture is selenium-rich, and to the left where p has values less than zero the mixture is metal-rich. Deviations of the alloy composition from the stochiometric point are of interest. Strauss (Ref. 7) points out "In samples which have not been intentionally doped, the electrical conductivity is due primarily to electrons or holes produced by the ionization of donor or acceptor lattice defects associated with deviations from stochiometry." This feature is of particular importance in the reduction of ionized defects using the method of isothermal annealing which will be explained in Section III.

When source materials of stochiometric proportions of $Pb_{0.9}Sn_{0.1}Se$ were deposited onto fluoride and alkali halide substrates, the resulting films always showed a deviation from stochiometry on the selenium-rich side. Hoff (Ref. 8) attributes this primarily to lattice site vacancies of metal atoms within the crystal structure which result in a net increase of two free hole carriers per metal vacancy, or a p-type semiconductor. The purpose of the annealing phase is to provide metal-rich compensation in order to reduce the number of free hole carriers. The temperature-composition diagram shows that the solidus region occurs to a limited extent on either side of the stochiometric axis. Pure crystalline form is possible only within this solidus region, and this determines the range of possible deviations from

stochiometry within which it is possible to fabricate Pb-Sn-Se semiconductors (Refs. 8, 9).

B. BAND INVERSION MODEL OF $Pb_{1-y}Sn_ySe$

The band inversion model which was originally proposed by Dimmock et al (Ref. 10) to explain the variation in energy-gap with composition and temperature of $Pb_{1-x}Sn_xTe$ has subsequently been extended by Strauss (Ref. 7) to explain the behavior of $Pb_{1-y}Sn_ySe$. In this theory the valence and conduction bands of the pseudo-binary compound $Pb_{1-y}Sn_ySe$ approach each other as the ratio of Sn to Pb increases, thereby decreasing the energy-gap E_g. At some fixed ratio and temperature the two bands touch and the semiconductor becomes degenerate. As the amount of Sn is further increased, the bands invert and exchange roles. Figure 3 is a diagram of this band inversion model. The conduction and valence band extrema occur at the L^{-6} and L^{+6} points in the Brillouin zone, respectively, and are shown to approach each other, touch, and then invert as y increases. The L^{+6} state is now the conduction band and the L^{-6} state the valence band. Because the L^{-6} and L^{+6} states have only a two-fold spin degeneracy this material does not become a semi-metal at and beyond the inversion point, but remains a semiconductor with the valence and conduction bands interchanged (Refs. 1, 9, 10, 11). It is this feature of band-gap selectivity that has promoted significant interest in these semiconductors.

Figure 4 shows the variation in E_g with $0.0 \leq y \leq 0.4$ for $Pb_{1-y}Sn_ySe$ at four different temperatures (Ref. 7). For

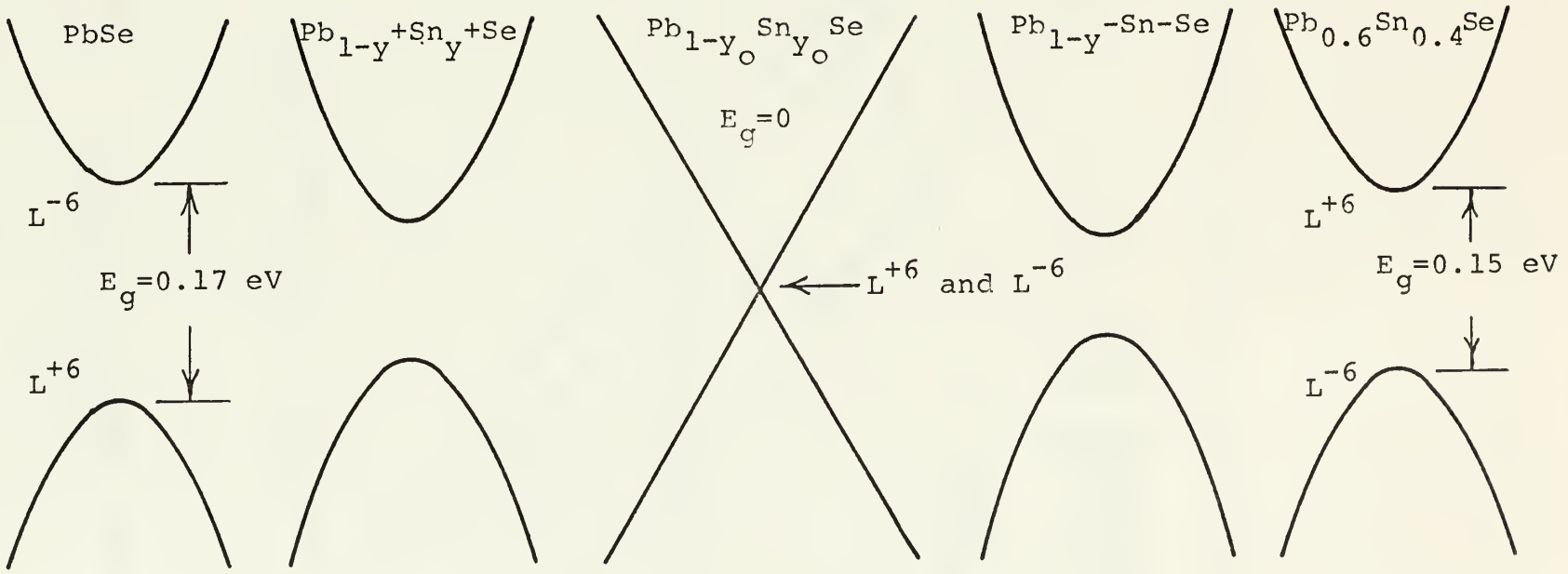

Figure 3. Schematic Representation of the Band Inversion Model for $Pb_{1-y}Sn_ySe$.

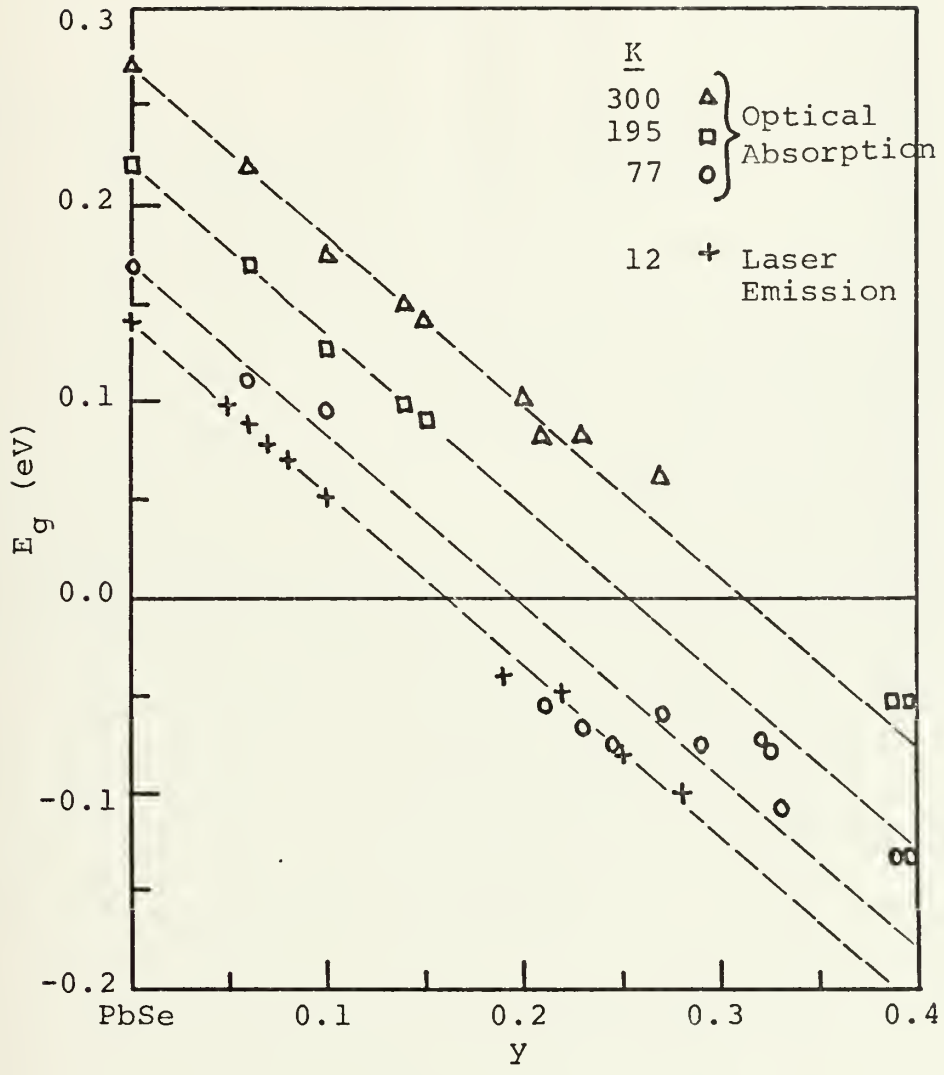

Figure 4. Variation of Energy Gap with y for $Pb_{1-y}Sn_ySe$.

y = .10 the E_g at 77°K is approximately .075 eV, or equal to a photon energy wavelength of 16 microns. The values of E_g plotted on these curves were obtained from both optical absorption data and from laser emissions from diode lasers made from Pb-Se and $Pb_{.96}Sn_{.04}Se$ (Refs. 7, 9).

III. PREPARATION OF SAMPLES

A. SEMICONDUCTOR PREPARATION AND THIN-FILM DEPOSITION

The semiconductors evaluated in this research consisted of thin-film $Pb_{0.9}Sn_{0.1}Se$ alloy which was deposited by vacuum evaporation techniques onto cleaved CaF_2 and BaF_2 substrates.

1. Preparation of Source Materials

The source materials used were 99.9999 per cent pure Pb and Sn obtained commercially from Cominco, Inc. and 99.999 per cent pure Se purchased from American Smelting and Refining Co. As discussed in Section II, the ratio of PbSe and SnSe determines the energy-gap of the pseudo-binary semiconductor alloy $Pb_{1-y}Sn_ySe$. This research was primarily concerned with the composition y=0.10.

Stochiometric molar quantities of Pb, Sn, and Se were measured using an analytical balance and placed in a clean quartz ampoule. For the composition y=0.10 stated, the weight ratio of each material was

Pb	55.96 grams
Sn	3.56 grams
Se	23.69 grams

The ampoule was then evacuated to a pressure in the mid-10^{-6} torr range. It was then sealed inside a slightly larger quartz tube which was back-filled with helium gas. The purpose of this outer jacket was to prevent contamination

of the source materials in the event of cracking of the inner ampoule during the sudden quenching step. The double ampoule was placed in a regulated furnace, and the temperature was slowly raised to a temperature of 1050°C, which is approximately 20°C above the melting point of this alloy composition (Ref. 7). The melt was kept at this temperature for 24 hours and then rapidly quenched in water. In addition to the preparation of this stochiometric alloy, a metal-rich mixture consisting of 52% metal and 48% chalcogenide was prepared in the same manner as discussed above. It was used in the annealing step to provide a metal-rich vapor. Following the quenching, the ampoules were opened and the alloy ingot was crushed into small pieces and stored in a desiccator box.

2. Preparation of the Substrate

The materials used as substrates were single crystal CaF_2 and BaF_2 obtained from Harshaw, Inc. They were chosen over the alkali halide crystals such as NaCl and KCl because of their ability to survive the annealing temperatures up to 600°C, and also because of their adequate transmission in the 2 to 16 microns region. A short time prior to deposition these crystals were cleaved using a sharp blade. The cleavage plane was (111) which was perpendicular to the long axis of the purchased crystal. The resulting substrates were in the form of a thin disk approximately 12.5 mm in diameter by 4 mm thick. They were then carefully inspected for fractures and excessive cleavage steps. Following this, they

were mounted in a stainless steel substrate holder for the deposition. The purpose of this holder was to position the substrates within the deposition chamber. It had space for seven substrates, six of which were used for samples and one for the mounting of a thermocouple to measure and control the substrate temperature during deposition. A mask was used in front of each substrate. Masks of two different shapes were used, one for the Hall samples, the other for optical samples.

After the substrates and thermocouple had been mounted, the rack was placed upon a stand located in the vacuum deposition chamber of a Varian/NRC vacuum deposition system. This stand positioned the substrates approximately 14 cm above a crucible or "boat." Boats of both alumina and graphite were used in the depositions reported here. Located between the boat and the substrate holder was a flat metal shutter which could be rotated from outside the evacuated chamber. The boat was heated by passing a d.c. current through a tungsten wire basket surrounding the boat. In order to heat the substrates, a tantalum strip heater was placed above the substrate holder. This heater was controlled by a Barber-Coleman temperature controller which maintained a constant temperature accurate to 2-3°C. The substrate temperature is an important factor in the preparation of high quality alloy films. The relationships between various deposition parameters and their effect on the crystal properties of the thin-film samples are mentioned in Section IV.

3. One-Boat Vapor Deposition Procedure

The previously prepared $Pb_{0.9}Sn_{0.1}Se$ alloy was deposited onto the substrates using the one-boat method described by Tao and Wang (Ref. 4). The method was employed as follows.

Several grams of the crushed alloy were placed in the boat which was positioned below the substrate holder. When the graphite boat was used a molybdenum sheet having a 1/16 in. aperture was placed over it. No aperture was used with the alumina boat. When all the interior components were in place, the vacuum bell jar was lowered onto its sealing flange and the chamber was evacuated to a pressure in the low-10^{-6} torr range using both a mechanical vacuum pump and a six inch diffusion pump. The boat was heated by passing a current of approximately 55 to 60 amps through the heating basket surrounding the boat. Figure 5 shows the deposition chamber and power supply. The alloy sources was heated to temperatures in the range of 740 to 280°C for the various samples prepared for this research. As a result of the high alloy temperature and the extremely low pressure within the bell jar, evaporation took place. The substrate heater was started prior to the boat heater because of its slower heating rate. Upon reaching the desired substrate temperature the evaporation was run for several minutes to attain steady-state. The shutter was then opened for a period of time varying from 15 to 30 minutes permitting the alloy vapor to condense upon the substrate and form a thin film. The deposition rates varied between 500 and 1800 Å/min. The

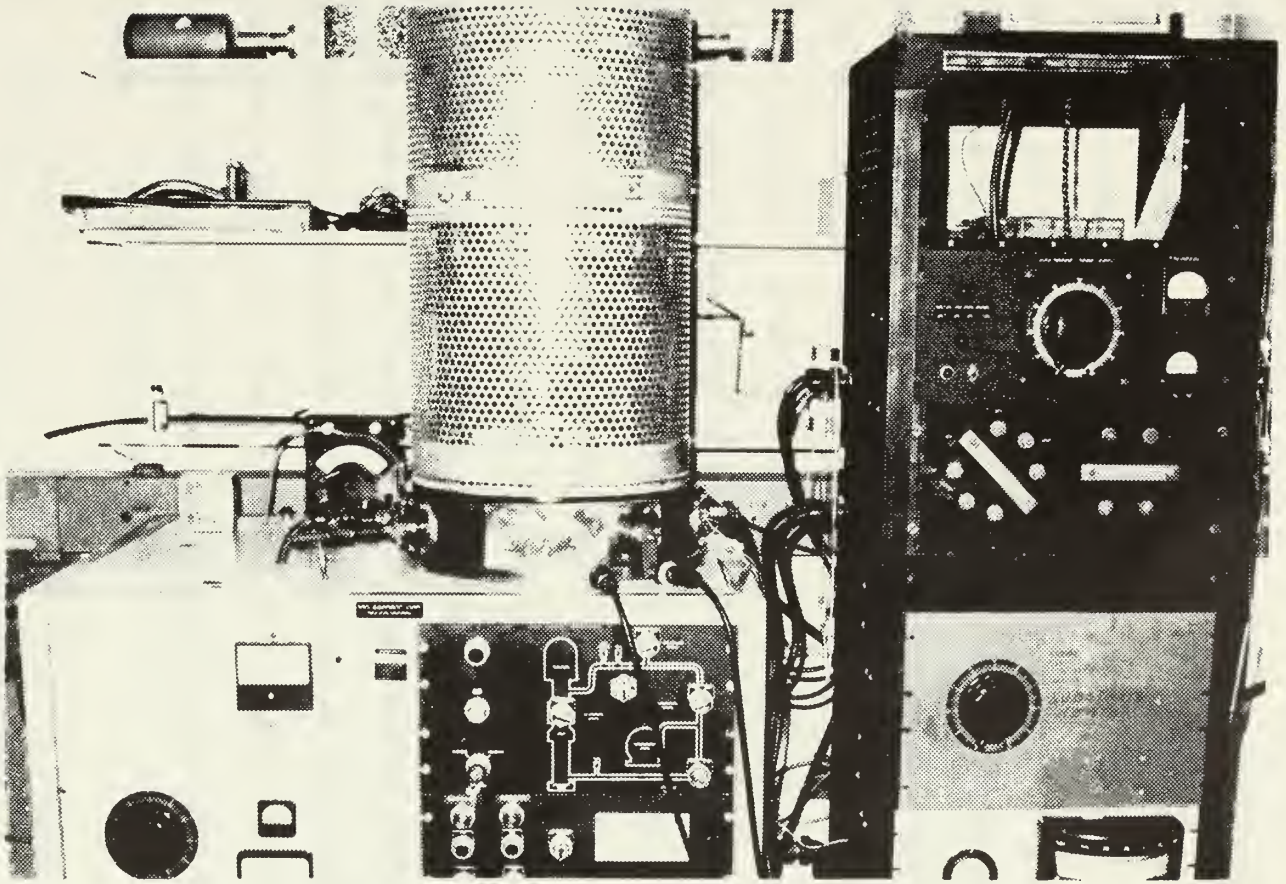

Figure 5. Vacuum Deposition Chamber and Power Supply.

film thickness can be estimated from the deposition rate and the time which the shutter is open. Table III lists the deposition parameters and the resultant crystal structures for the samples which were used in this research. The film thickness listed was measured using methods described in Section IV, and from this information and the deposition time, a deposition rate was obtained. This rate is only approximate, and can be highly inaccurate in some cases due to differences in deposition rates caused by non-uniform boat temperatures, premature evaporation of the source material before the allotted deposition time was completed and other factors. Once the desired thickness was achieved, the shutter was closed and the boat and substrate heaters were shut down. The chamber was left to cool for approximately three hours before opening. The substrate holder was then removed and the substrates taken out. The entire chamber, including all of its components were then thoroughly cleaned to prevent contamination in succeeding depositions. The samples were placed in individual boxes and were marked with an identification number which designated the thin-film type, composition, boat type, deposition run, and sample i.d. number. An example is

SS-10-K-11-3

where SS indicates Pb-Sn-Se, 10 indicates 10% SnSe, K is the boat type (K is a graphite Knudsen boat, OB is an alumina open boat), and 11-3 stands for deposition 11, sample #3.

TABLE III

DEPOSITION PARAMETERS FOR $Pb_{0.9}Sn_{0.1}Se$

Sample Number	Substrate	Boat Temp (°C)	Substrate Temp (°C)	Deposition Time (min)	Film Thickness (μ)	Rate (Å/min)	X'tal Structure
SS-10-OB-7-3	CaF2	750	325	15	2.18	1455	PC(100)+(111)
SS-10-OB-7-4	CaF2	750	325	15	2.18	1455	PC(100)+(111)
SS-10-OB-8-3	CaF2	750	325	15	2.66	1770	PC(100)+(111)
SS-10-OB-8-4	CaF2	750	325	15	2.75	1840	PC(100)+(111)
SS-10-OB-10-2	CaF2	740	285	15	.95	635	SC(100)
SS-10-OB-10-3	CaF2	740	285	15	.95	635	SC(100)
SS-10-OB-10-4	CaF2	740	285	15	.99	660	SC(100)
SS-10-OB-11-1	CaF2	780	325	20	2.3	1150	SC(100)
SS-10-OB-11-2	CaF2	780	325	20	1.93	965	SC(100)
SS-10-OB-11-3	CaF2	780	325	20	2.02	1020	SC(100)
SS-10-OB-11-5	CaF2	780	325	20	2.00	1000	SC(100)
SS-10-OB-12-3	BaF2	780	200	20	1.13	755	SC(111)
SS-10-OB-12-4	BaF2	780	300	15	.93	620	SC(111)
SS-10-OB-12-5	BaF2	780	300	15	.93	620	SC(111)
SS-10-OB-13-2	CaF2	780	300	15	.80	533	PC(100)+(111)
SS-10-OB-13-3	CaF2	780	300	15	.94	625	PC(100)+(111)
SS-10-OB-13-4	CaF2	780	300	15	.87	680	PC(100)+(111)
SS-10-OB-13-5	CaF2	780	300	15	.76	506	PC(100)+(111)
SS-10-K5-3	CaF2	810	270	30	3.40	1130	PC(100)+(111)
SS-10-K5-4	CaF2	810	270	30	3.57	1130	PC(111)+(111)
SS-10-K6-2	CaF2	820	310	25	2.89	1430	PC(100)+(111)
SS-10-K6-3	CaF2	820	310	25	2.84	1430	PC(100)+(111)

Thin films deposited by this method were generally shiny in appearance and showed good adhesion to the substrate. Most were free of major surface imperfections, although some showed prominent cleavage lines or pin holes. It is possible that the cleavage steps affected the carrier mobilities by increasing the number of scattering sites (Ref. 13). The effect of the pin holes has not been investigated, although several samples having pin holes had good photoconductive responsivity (Ref. 14). The samples were stored in a desiccator when not being used, and utmost attention was given to maintaining the cleanliness during handling.

B. ISOTHERMAL ANNEALING

The purpose of the isothermal annealing step was to reduce the carrier concentration of the as-deposited films in order to improve the photoconductive properties. Isothermal annealing techniques were first applied to PbTe by Brebrick and Allgaier (Ref. 15). Since then, isothermal annealing has successfully been applied to $Pb_{1-x}Sn_xTe$ and $Pb_{1-y}Sn_ySe$.

1. Principle of Isothermal Annealing

Isothermal annealing involves the equilibration of a metal-rich or chalcogenide-rich vapor of alloy composition y with a Pb-Sn-Chalcogenide crystal of composition y, but with a controlled initial defect concentration (Ref. 16). As was stated in the first section, the defects in the as-deposited thin films were considered to be primarily metal vacancies and/or excess chalcogenides within the crystal

structure. Unannealed samples of $Pb_{0.9}Sn_{0.1}Se$ which were measured by Wang (Ref. 17) had p-type carrier concentrations which ranged between low $10^{18}cm^{-3}$ to high $10^{17}cm^{-3}$. Figure 6 is an annealing temperature and non-stochiometry diagram for $Pb_{0.9}Sn_{0.1}Se$. It has been established that the boundary of the solidus field crosses the line representing the stochiometric composition at two values of annealing temperature T. The points T_h and T_l indicate the temperature where the alloy is stochiometric and where the carrier concentration should approach its lowest, or intrinsic value. Alloys whose stoichiometry falls within the solidus field, and to the right of this line contain defects which produce a net p-type concentration (selenium-rich side), while those on the left side of the line result in n-type carriers (metal-rich side). The unannealed samples prepared for this research were mostly p-type.

By supplying a metal-rich vapor and by properly selecting an annealing temperature T_{ann} it is possible to arrive at an equilibrated state along the solidus line either on the p or on the n side. If the temperature is held constant at T_h or T_l for a long enough time for the alloy to reach equilibrium, the initial defect concentration can be reduced theoretically to the intrinsic level. Any temperature greater than T_l and less than T_h will result in n-type films. Since the thin film samples cannot withstand excess sublimation during annealing, it was decided to determine experimentally the lower stochiometric temperature T_l. Some

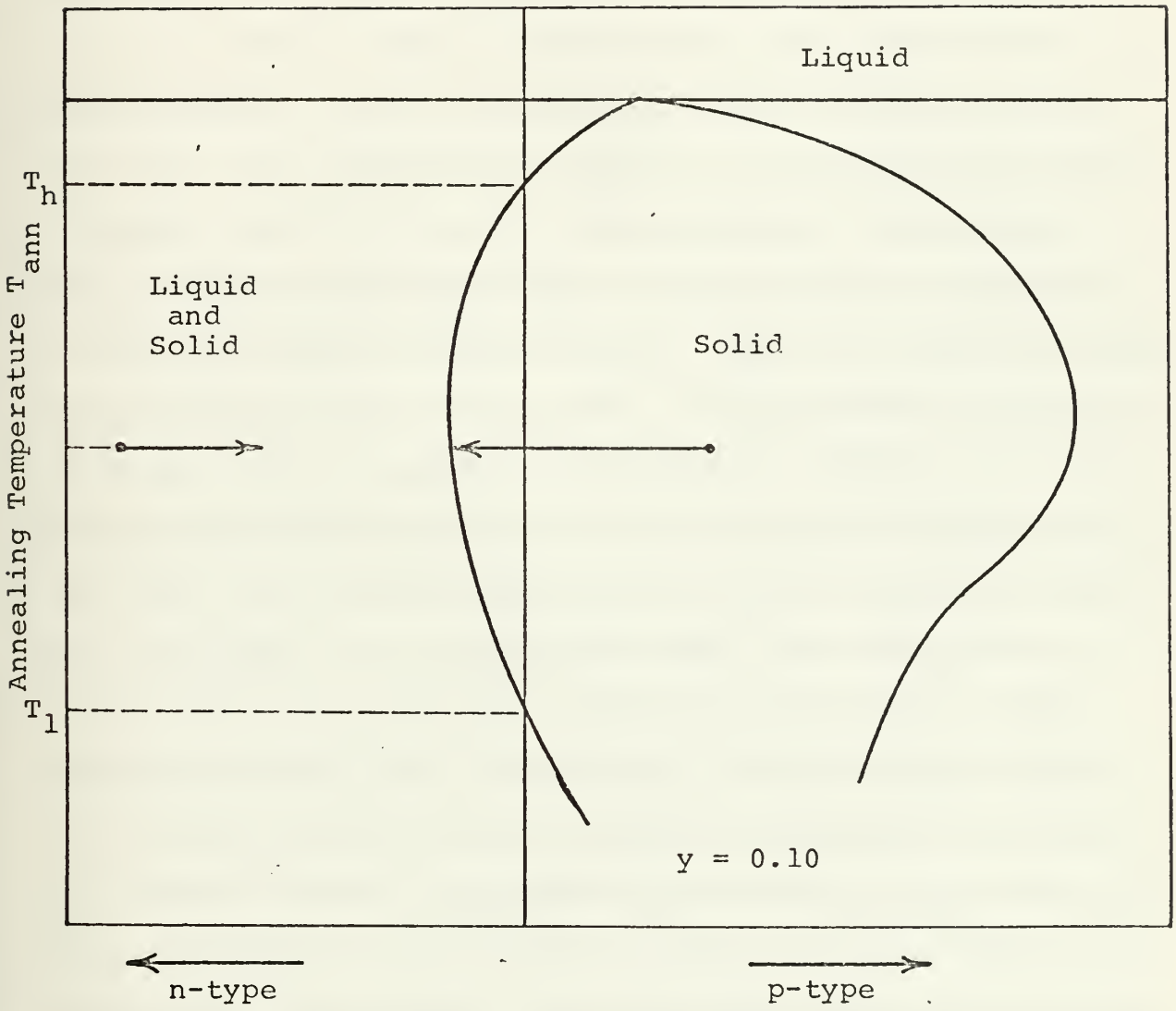

Figure 6. Annealing Temperature and Non-Stochiometry Diagram for $Pb_{0.9}Sn_{0.1}Se$.

preliminary research had been done by Wang (Ref. 17) in determining this temperature for $Pb_{0.9}Sn_{0.1}Se$.

2. Annealing Procedure

Special annealing ampoules were made of 7/16 in. quartz tube. These ampoules were divided into two chambers separated by a narrow indentation and were approximately 8 in. in overall length. The ampoules were first chemically etched using a solution of fifty per cent nitric acid and fifty per cent hydrofluoric acid in a Cole-Palmer ultrasonic cleaning tank for 24 hours. After etching, the ampoules were rinsed in deionized water for several minutes and then rinsed with double-distilled water. They were then air dried in an oven at 200°C for 1/2 hour. These cleaning steps were done as closely as possible to the actual annealing in order to prevent contamination of the quartz. Upon removal from the oven, the ampoules were scribed with an identifying number and placed in a laminar-flow hood. The semiconductor samples were then carefully washed in spectroscopic grade acetone and dried with nitrogen gas. Several small chunks of the metal-rich alloy was placed in one end of the annealing ampoule and the two samples were placed in the other end. The indentation of the quartz tube wall prevented the samples from coming into contact with the metal-rich source materials as long as the ampoule was not inverted.

A wet paper towel was then wrapped around the lower portion of the ampoule and a thin neck was drawn in the upper portion of the ampoule by heating the quartz with a hydrogen torch. The wet towel prevented the heat from affecting the

samples and also allowed the ampoule to be hand-held during the quartz sealing operation. The ampoules were then allowed to cool to room temperature. When cool enough to handle, the ampoules were avacuated and then backfilled with helium gas utilizing the Varian/NRC vacuum system. Each ampoule was evacuated and purged with helium gas several times and then sealed using a hydrogen or acetylene torch. The sealing generally took place when the helium back-pressure was about .1 torr. This pressure of helium was chosen to help prevent excessive sublimation of the thin film during annealing and to provide an inert atmosphere around the samples and source material. No excessive sublimation was noted in $Pb_{0.9}Sn_{0.1}Se$ when this method was used. Figure 7 shows a sealed ampoule containing the metal-rich source material and two samples.

The isothermal annealing was accomplished using four furnace-controller combinations. After a short period of time it became obvious that only two of the controllers were stable enough to yeild good results. The two good combinations consisted of Marshall Model 1024 furnaces controlled by Marshall proportional controllers. The accuracy of temperature regulation was stated by the manufacturer to be ±1°C. These good furnaces were numbered two and three. Figure 9 is a photograph of one of the annealing stations showing the annealing furnace and controller. The unsatisfactory combinations consisted of Marshall 1024 furnaces controlled by a modified API proportional controller in one case and a Wheelco-Sloan on-off controller in the other. The API controller failed completely and the Wheelco-Sloan

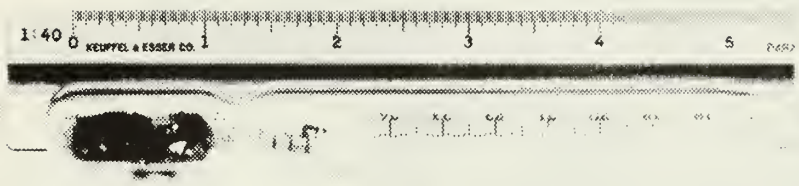

Figure 7. Annealing Ampoule Showing Samples, and Source Material.

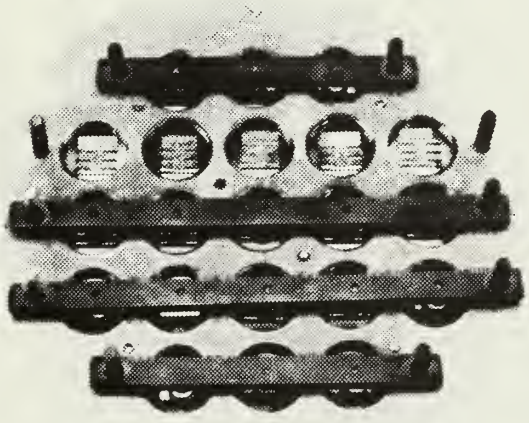

Figure 8. Substrate Holder Used in Deposition of Gold Films.

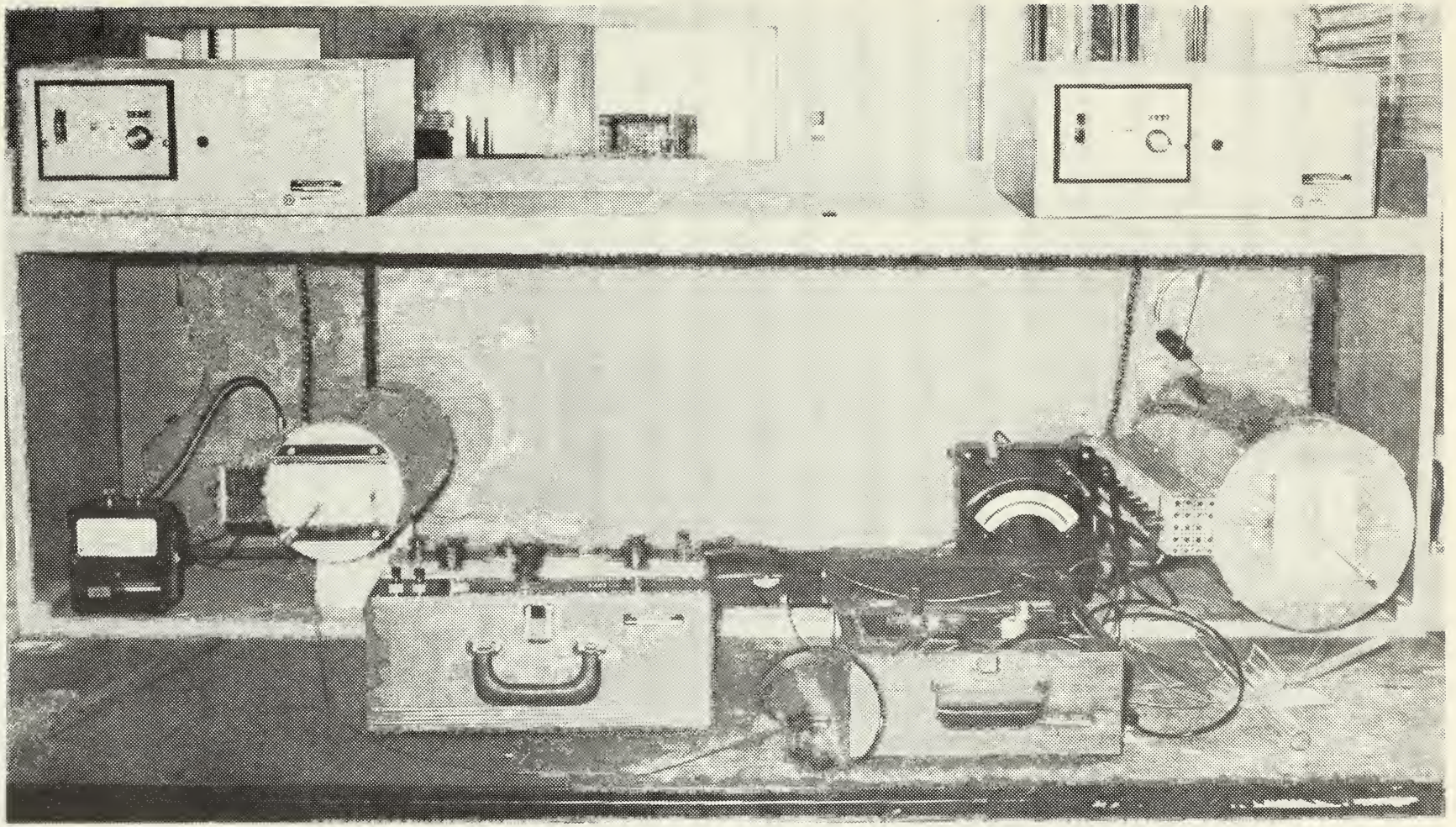

Figure 9. Annealing Stations.

exhibited erratic regulation a large part of the time. These ovens were numbered one and four, respectively. Prior to any annealing, a temperature profile was measured for each furnace in order to locate the position of flat temperature zones along the tubular furnace. These flat zones averaged five cm in length and the two samples to be annealed were positioned within this zone. The flat zone temperature was monitored by means of a chromel-alumel thermocouple inserted through the front of the furnace door. This thermocouple was encased in a quartz sleeve to prevent bending. Spot checks of the annealing temperature in each oven were made at various times during the annealing and any significant deviation from the desired tempeaature was recorded and corrected by adjusting the controller.

At the completion of the selected annealing time, the samples were removed from the ovens in several steps. First, the ampoule was moved to the oven door and allowed to settle for several minutes. It was then moved halfway out of the door for another minute. Finally, it was completely removed from the oven and cooled to room temperature. The reason for these steps was to minimize the thermal shock on the substrate and film. Whether it changed the annealing conditions or not is open to question, although it is unlikely considering the very short times involved. The actual annealing temperature was arrived at based upon the temperature data recorded during the spot checks. If at any point the recorded temperature varied significantly higher

than the desired temperature and remained there for periods exceeding fifteen or twenty minutes, this new temperature was considered the annealing temperature for the sample. Due to erratic functioning of two of the controllers an accurate temperature could not be determined for some of the samples. These inaccuracies are noted in Table IV.

The experimental procedure used in determining the annealing can be summarized as follows. A "best guess" starting temperature was selected based upon data from other studies (Refs. 8, 17) and from previous anneals. The carrier type, mobility, and concentration were then determined using techniques outlined in Section IV. This information was then fed back to the succeeding anneals, thereby gradually bracketing the temperature T_1. The best estimate of the lower temperature T_1 is 319.5°C. Samples which were annealed at 319.75°C and above exhibited n-type carrier concentrations, while those annealed below 319.5°C were p-type. Table IV lists the annealing temperatures of all samples as well as some of their pertinent electrical characteristics. In several of the cases, either the temperature control of the annealing ovens was poor which resulted in a temperature drift, or insufficient annealing time was used. The results on these samples deviated from the expected values, and are noted in the table. In addition, several of ampoules contained one sample of n-type and one sample which was p-type after annealing. This was possibly caused by one of the samples being partially covered

TABLE IV

ELECTRICAL PROPERTIES OF ANNEALED $Pb_{0.9}Sn_{0.1}Se$ SAMPLES

Sample Number	Thickness (μ)	X'tal Structure	Temp (°C)	Carrier Concentration (cm^{-3})	Mobility (cm^2/V-sec)
SS-10-OB-7-3 CaF_2	2.18	PC(100)+(111)	310.5[a]	1.48×10^{17}(p)	1040
SS-10-OB-7-4 CaF_2	2.18	PC(100+(111)	310.5[a]	1.30×10^{17}(p)	4230
SS-10-OB-8-3 CaF_2	2.66	PC(100)+(111)	312[b]	7.82×10^{16}(p)	6210
SS-10-OB-8-4 CaF_2	2.75	PC(100)+(111)	312[b]	6.93×10^{16}(p)	7350
SS-10-OB-10-2 CaF_2	.95	SC(100)	310	5.66×10^{17}(p)	77
SS-10-OB-10-3 CaF_2	.95	SC(100)	317[c]	1.06×10^{17}(p)[e]	468
SS-10-OB-10-4 CaF_2	.99	SC(100)	317[c]	1.11×10^{17}(p)	504
SS-10-OB-11-1 CaF_2	2.3	SC(100)	319.75	2.20×10^{18}(p)	997
SS-10-OB-11-2 CaF_2	1.93	SC(100)	303[d]	4.90×10^{16}(p)	139
SS-10-OB-11-3 CaF_2	2.02	SC(100)	303[d]	5.14×10^{16}(p)[e]	134
SS-10-OB-11-5 CaF_2	2.00	SC(100)	324	4.73×10^{17}(n)	1600
SS-10-OB-12-3 BaF_2	1.13	SC(111)	321	5.42×10^{17}(n)	857
SS-10-OB-12-4 BaF_2	.93	SC(111)	313	2.29×10^{17}(p)	5950

TABLE IV (Continued)

Sample Number	Thickness (μ)	Structure	Temp (°C)	Carrier Concentration (cm^{-3})	Mobility (cm^2/V-sec)
SS-10-OB-12-5 BaF_2	.93	SC(111)	313	2.29×10^{17}(p)	29200[i]
SS-10-OB-13-2 CaF_2	.80	PC(100)+(111)	320	1.56×10^{18}(p)	22
SS-10-OB-13-3 CaF_2	.94	PC(100)+(111)	320	3.12×10^{17}(n)	920
SS-10-OB-13-4 CaF_2	.87	PC(100)+(111)	312[g]	3.75×10^{17}(p)	27.7
SS-10-OB-13-5 CaF_2	.76	PC(100)+(111)	312[g]	4.34×10^{17}(n)	123
SS-10-K5-3 CaF_2	3.40	PC(100)+(111)[f]	319.5	4.83×10^{17}(p)	1450
SS-10-K5-4 BaF_2	3.57	PC(111)+(100)	319.5	4.88×10^{17}(p)	4397
SS-10-K6-2 CaF_2	2.83	PC(L00)+(111)	319.5	2.20×10^{18}(p)	10.4
SS-10-K6-3 CaF_2	2.84	PC(100)+(111)	316.5[h]	7.35×10^{16}(p)	36.4

Notes: a: Removed from oven in 30 hours. All other samples annealed 96 to 120 hrs.
b: 308 to 309°C average temp.
c: Excellent oven regulation.
d: Very poor oven regulation. Max. temp. higher.
e: High temp. Hall reversal.
f: Laue indicates SC, diffractometer-PC.
g: Temp. up to at least 315°C. Poor reg.
h: Raised intentionally to 324°C.for 20 min.
i: Low temp Hall reversal.

by the other and thereby not fully exposed to the metal-rich vapor. These samples are also noted in the table. Figure 10 shows the variations in 90°K carrier concentration and carrier type as a function of annealing temperature.

3. Deposition of Gold Contacts

In order to make electrical connections to the thin films it was necessary to deposit a thin layer of metal on selected areas of the samples. Gold was used in this research, and the deposition of this metal onto the alloy films was done also in the Varian-NRC deposition chamber.

a. Pre-Deposition Cleaning

Several steps were taken to ensure successful adherence between the semiconductor film and the deposited gold layer. These steps were primarily concerned with maintaining the cleanliness of both the sample and the deposition apparatus. Sample cleanliness was achieved by keeping the samples sealed inside the annealing ampoules until just prior to the deposition step. The inert helium gas within the ampoules prevented contamination of the annealed films from the outside environment. During handling of the annealing ampoules, precautions were taken to prevent the metal-rich source material in one end of the quartz tube from coming into contact with the pair of samples in the other end. Caution was also given to prevent the samples from rubbing against each other.

Upon opening the sealed ampoules, the samples were inspected for annealing damage and placed in a gold

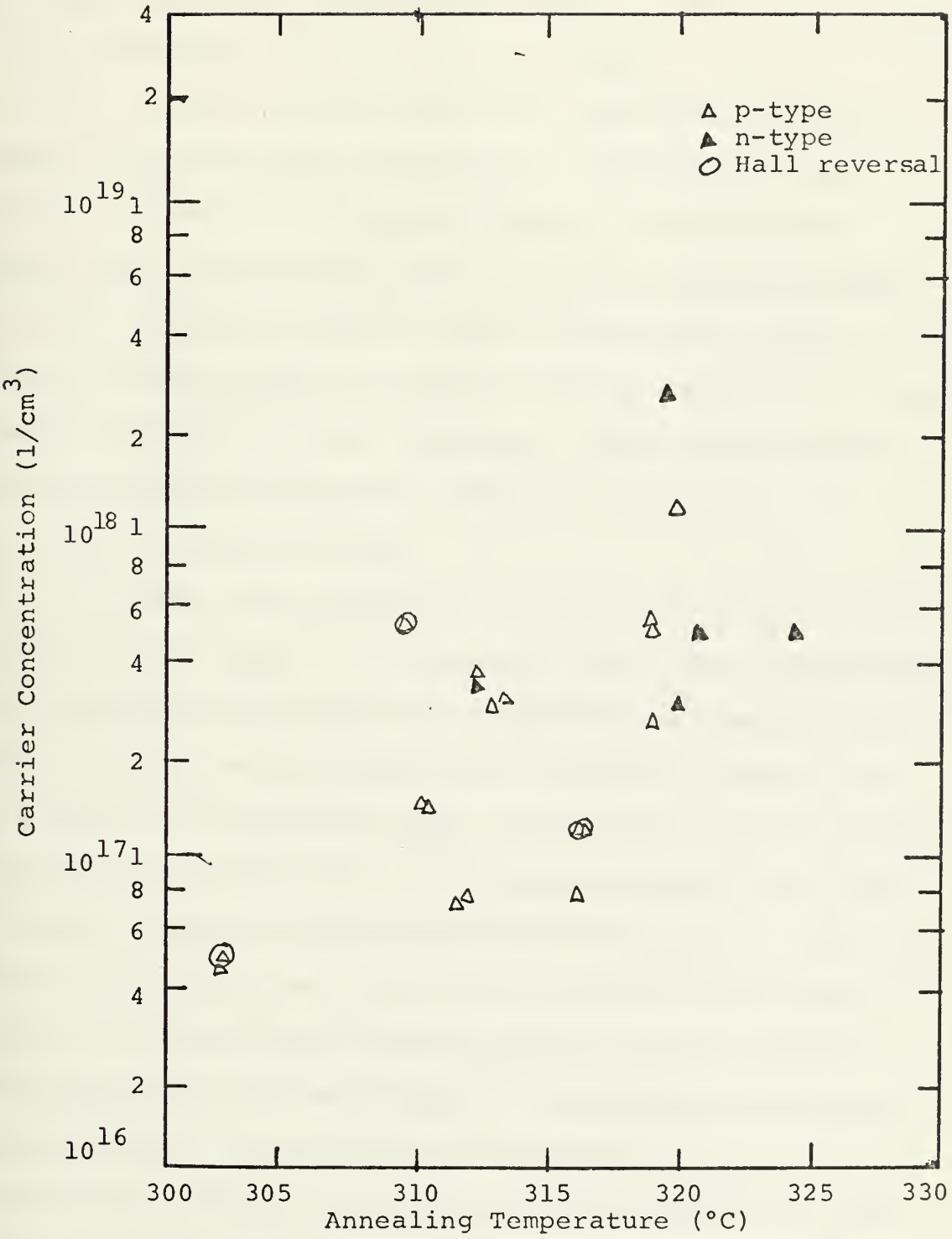

Figure 10. Variation of 90°K Carrier Concentration with Annealing Temperature.

deposition holder. This holder contained spaces for twenty-one samples and incorporated masks which defined the area for gold deposition over a portion of the thin film. Figure 8 is a photograph of this substrate holder.

Prior to gold deposition the entire deposition chamber and associated equipment was thoroughly cleaned to prevent contamination from the residue of any previous depositions. After this initial cleaning the chamber was baked for a period of two or three hours under vacuum. The purpose of this step was to drive off any contaminants which remained after the initial cleaning. This baking step was done periodically during the period of research.

b. Gold Deposition

The gold deposition was done in a manner similar to that used in depositing the alloy film. The clean samples were loaded into the holder and carefully aligned with the masks. 99.9999 per cent pure gold, purchased from R.I.C. was placed in a molybdenum boat. The holder containing the samples was supported on a stand approximately 20 cm above the boat. A glass cylinder surrounded the boat in order to prevent the deposition of gold on the rest of the vacuum chamber. A shutter was located between the boat and the substrate holder for the purpose of externally controlling the deposition. The substrates were heated by means of a tantalum-wire heater placed on top of the holder. The temperature of the substrates was measured using a copper-constantan thermocouple which was placed in a vacant substrate

cell in the holder. The output of this thermocouple was fed to a Barber-Coleman temperature controller which maintained a constant substrate temperature during the deposition.

When all the components were in place, the bell jar was lowered and the chamber was evacuated to approximately 2×10^{-6} torr using the diffusion pump. The substrate heater was set to 150°C and turned on to allow warm-up. The shutter was then closed and the current through the boat was gradually raised to around one-hundred amperes, at which point the boat was white hot. After several minutes a steady-state condition was reached and the shutter was opened, allowing deposition to begin. Thesystem was shut down at the end of the deposition time and the apparatus was cooled to room temperature before removal of the substrates. The samples were then inspected for adhesion and flaws and returned to the desiccator. Deposition times of from ten to fifteen minutes were used and resulted in gold film layers which had high luster, and generally good adherence to the alloy film and to the substrate.

c. Application of Electrical Leads

The final step in sample preparation was attaching the wire leads to the semiconductor sample. All of the samples evaluated in this research have the conventional Hall configuration shown in Figure 11, and require a total of eight wire leads. The samples used for photoconductive measurements required removal of the six side leads, but keep the end leads intact.

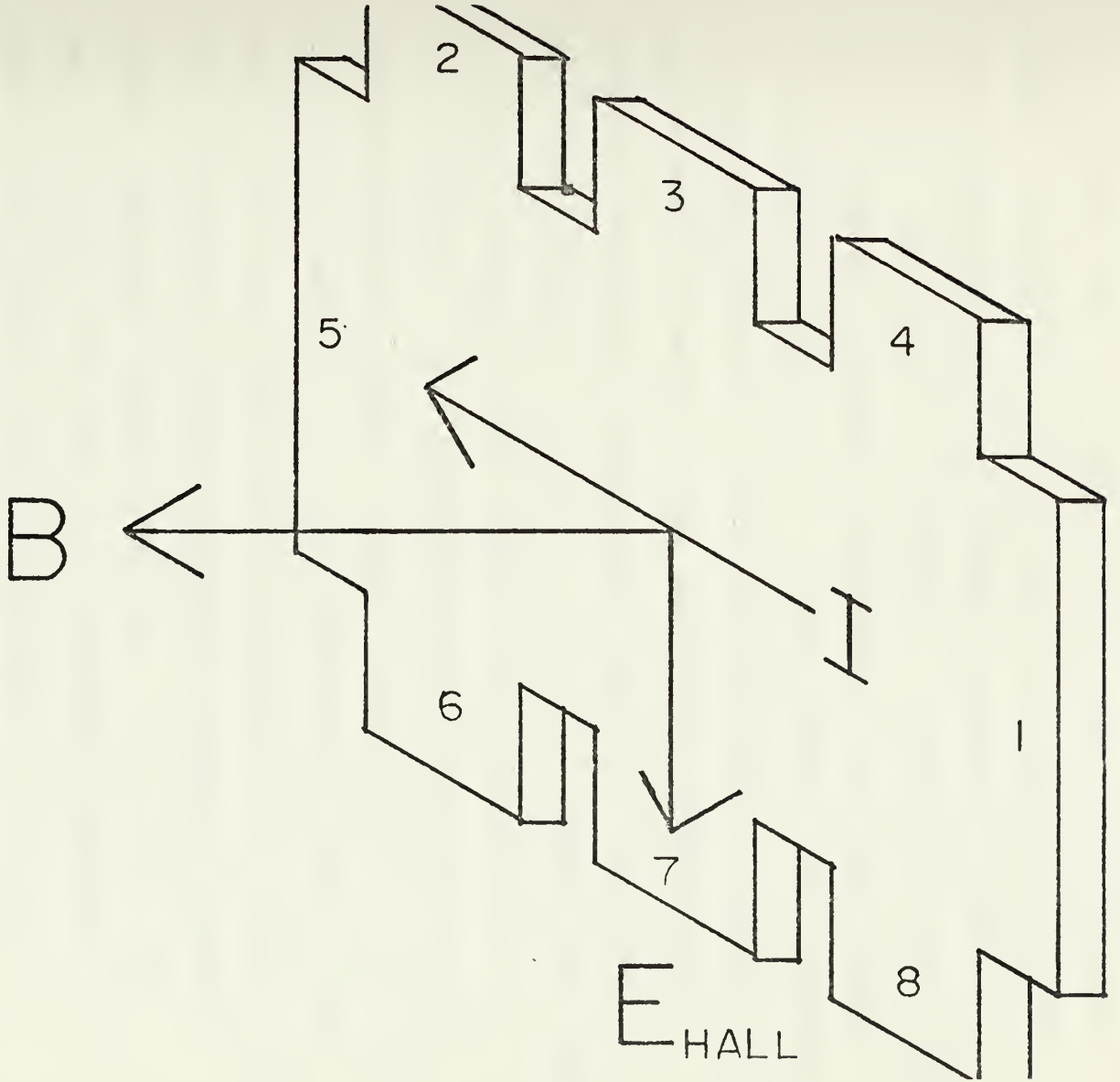

Figure 11. Configuration of Typical Hall Sample.

Many different methods of attaching the leads to the gold contacts have been used in other research (Refs. 8, 17, 18). The silver-epoxy bonding method was chosen in this case because of its ease of preparation, strength, and availability. The wire used for the leads was size 25/44 copper wire made by the New England Electric Works, Inc. This wire was cut into leads one inch long and cleaned with acetone. A freshly prepared mix of silver-epoxy E-Solder 3021 manufactured by Epoxy Products Company was applied to the sample where leads were desired. One end of a wire lead was then coated with epoxy and joined to the epoxy already on the sample. Approximately fifteen minutes were required to fasten the eight wire leads to each sample. Usually two samples could be prepared with each batch of epoxy before hardening occurred. The epoxy was kept under refrigeration when not being used in order to extend its useful life, and to allow a slightly longer working time once the mix had been prepared. It was determined from experience that the samples should be airdried at room temperature for from four to six hours before use. Some samples were dried on a hot plate at 60°C and these proved unsuccessful when cycled from 300 to 90°K due to contact separation problems occurring between the alloy and the substrate. It is likely that these problems were caused by a too rapid hardening of the epoxy which caused a slight contraction of the epoxy-gold junction upon cooling and subsequent separation. The contact adhesion was generally good when cured at room

temperature and when the surfaces were clean. The contact resistance was high in several of the samples and was believed to have been caused by contaminated epoxy.

IV. EVALUATION OF SAMPLES

A. METALLURGICAL PROPERTIES AND MEASUREMENTS

All thin film samples underwent three measurements to determine film thickness, crystal structure, and crystal orientation. Thickness measurements were made using optical interferometric methods. The crystal structure was determined from Laue back-reflection photographs, and the crystal orientation was obtained by the analysis of X-ray diffractometer scans.

1. Determination of Thin Film Thickness

The samples were mounted in the source side of a Perkin Elmer Model 137B Infrared Spectrophotometer, and a plot was made of film transmission versus wavelength. The region scanned was between 2.5 and 16 microns. For samples whose carrier concentration was lower than $10^{19} cm^{-3}$, this transmittance versus wavelength plot exhibited interference fringes. By measuring the difference between subsequent peaks, an estimate of the film thickness can be made by using the formula (Ref. 17)

$$d = \frac{\Delta k_{\nu}}{2n(\nu_{(i+k)} - \nu_i)} \ (\mu) \qquad (1)$$

where d is the film thickness in microns, k is the number of intervals between the i^{th} and the $(i+k)^{th}$ transmission maxima, i and i+k are the wave number in cm^{-1} where the i^{th} and the $(i+k)^{th}$ transmission maxima occur, and n is the

index of refraction of $Pb_{0.9}Sn_{0.1}Se$ (n = 4.25). Table IV includes data on the thickness of thin film samples used in this research. The accuracy of the thickness measurements is estimated to be ten per cent, based upon possible calibration errors of the spectrophotometer, inaccuracies in interpreting the plots, and round-off errors in the calculations. In cases where thickness measurements of higher accuracy are needed, Wang (Ref. 17) discusses other methods.

2. Determination of Crystal Structure

Depending upon the deposition parameters, the resultant thin films can have either a single or polycrystalline structure (Ref. 11). A convenient method of determining the crystal structure is to obtain a Laue back-reflection photograph of the film. In this method, the $k\alpha_1$, $k\alpha_2$, and $k\beta$ X-ray radiation from a copper target is incident upon the thin film sample which is held stationary in a rigid mount. Only certain discrete wavelengths will be selected out and diffracted back to the film plane. Constructive reflections will occur only from those crystal planes whose spacing d' and incidence angle θ satisfy the Bragg equation

$$2d' \sin \theta = m\lambda \qquad (2)$$

where d' is the lattice spacing in Å, θ is the incidence angle, m is the order of the diffracted beam, and λ is the wavelength of the incident radiation (Ref. 11).

In a semiconductor with a single crystal structure the Laue photograph will show a symmetrical pattern of sharply defined spots caused by the constructive reflections

from the crystal planes which have a constant spacing and single orientation. Figure 12a shows a Laue photograph of a single crystal $Pb_{0.9}Sn_{0.1}Se$ sample deposited on CaF_2. When a polycrystalline structure occurs, the various orientations of the poly crystals within the film will cause the X-ray radiation to be reflected in a series of concentric rings, known as Debye rings (Ref. 11). Figure 12b shows a polycrystalline Laue photograph. In summary, the following criteria were applied to determine the crystal structure:

single crystal-sharp spots in Laue photograph. No Debye rings.

polycrystal-complete or broken Debye rings on Laue photograph.

3. Determination of Crystal Orientation

The third metallurgical measurement made on the thin film samples was one to determine the orientation(s) of crystal planes. This was done using a Norelco Model 12043 X-ray Diffractometer. The procedure was to focus the $k\alpha_1$, $k\alpha_2$, and $k\beta$ X-ray radiation obtained from a copper target onto the thin film, and to make a scan of the intensity of the diffracted radiation as a function of angle by moving the detector in a constant arc around the film. The location of these intensity peaks as a function of 2θ indicates the orientation of the planes causing the constructive reflections. It is also possible to use the diffractometer scans to obtain the lattice parameters of the crystal. Once

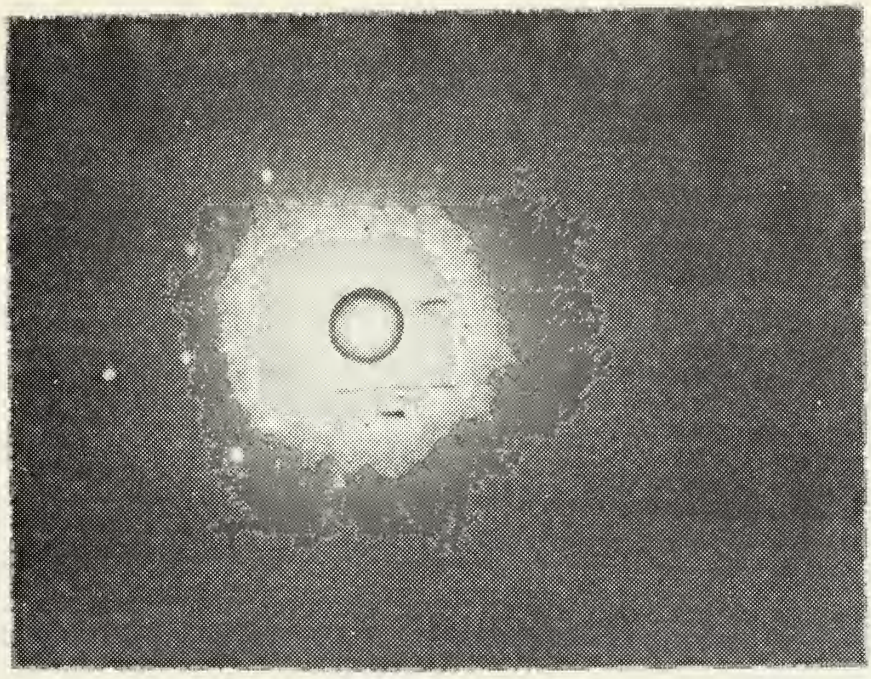

Figure 12a. Laue Photograph of Single Crystal Structure.

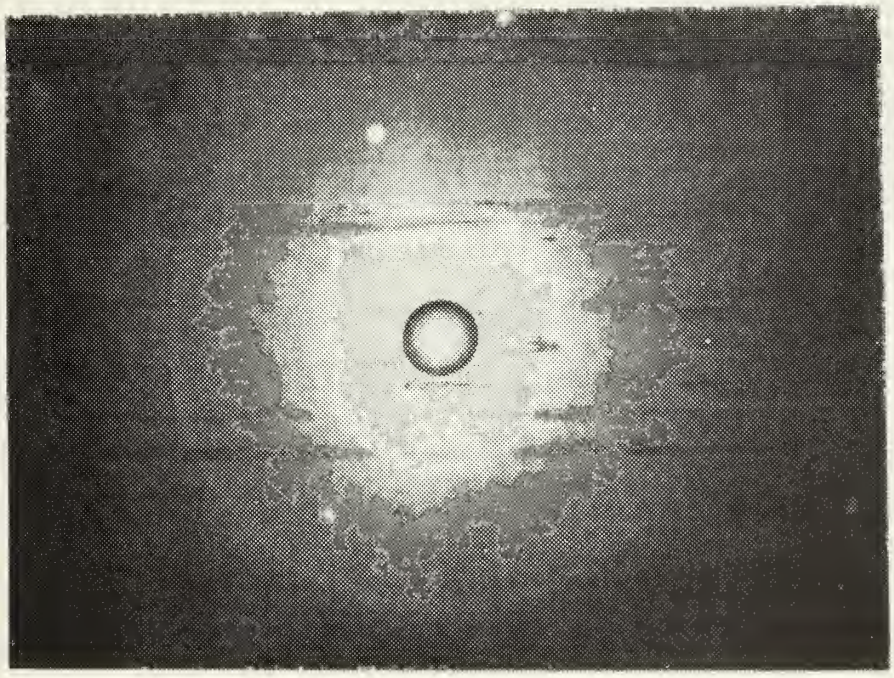

Figure 12b. Laue Photograph of Polycrystalline Structure.

these are available, the following Vegard relation can be used to calculate the alloy composition y (Ref. 7)

$$a(\text{Å}) = 6.127 - .12y \qquad (3)$$

where a is the lattice parameter obtained from the diffractometer scan, in Å, and y is the alloy composition for $0 \leq y \leq .43$. Previous research by Tao and others (Refs. 17, 18, 19) has shown that for thin films which have been deposited by the one-boat method, the alloy composition of the film is generally very close to the composition of the source material.

The orientation of the crystal planes appears to be an important factor in the photoconductive response of thin film $Pb_{0.9}Sn_{0.1}Se$ photodetectors, as well as in the low temperature mobilities of the free carriers to be discussed later in this report (Ref. 14). The film orientation was found to depend on the deposition parameters as well as on the orientation of the substrate, which in the cases of BaF_2 and CaF_2 is (111). The deposition parameters affecting the film orientation as well as the crystal structure are the substrate temperature and the deposition rate, which is a function of the boat temperature, boat aperture, and deposition time (Ref. 15). On samples which were deposited by the one-boat method, and on BaF_2 substrates heated to approximately 270°C during deposition, the resultant thin films were usually polycrystalline (111) + (100). When the substrate temperature was raised to 300°C, the films were found to be single crystal oriented in the (111) direction.

In the above cases the deposition rate was approximately 620 and 1130 Å/min. respectively. When CaF_2 was used as the substrate, a temperature of 325°C and a deposition rate of 1450 Å/min. resulted in polycrystalline films with a (100) preferred direction. By lowering the substrate temperature to 285°C and the deposition rate to 650 Å/min., single crystal (100) films were obtained. As is noted in the section on electrical measurements, the 90°K mobilities of these (100) CaF_2 single crystal films is very low. It is also interesting to note that subsequent photoconductive measurements of these low mobility samples yielded higher responsivities than films with other structure and orientations (Ref. 14). At this time, no single crystal (100) has been obtained on BaF_2, while both single crystal (100) and (111) can be deposited on CaF_2 (Ref. 19).

B. ELECTRICAL MEASUREMENTS

Electrical measurements were performed on all of the samples in order to determine the mobilities of the majority carriers and their carrier concentrations. Conventional d.c. Hall techniques were used in obtaining the conductivity voltage $V\sigma$ and the Hall voltage V_H at temperatures ranging between 300 and 90°K. From these measured values and other known data the majority carrier mobility $\mu_e(\mu_n)$ and the majority carrier concentration n(p) were calculated. In certain p-type samples whose hole concentration was close to the electron concentration, and whose Hall coefficient R_H

changed sign in the temperature range measured, a technique developed by Tao et al (Ref. 19) can be used to obtain the electrical properties of both the majority and minority carriers.

The mobilities for $Pb_{0.9}Sn_{0.1}Se$ samples at 90°K ranged from 20 to 29,000 cm^2/volt-sec. Majority carrier concentrations in the annealed samples varied between mid-10^{16} to low-10^{18} $1/cm^3$. Table IV lists the results of electrical measurements on all samples evaluated.

1. Hall Effect Summary

Figure 11 depicts the configuration of a typical Hall sample. A constant current I is passed through the sample from contact (1) to (5). In a semiconductor, this current will consist of negatively charged electrons which move with a velocity v in the direction opposite to the current flow and positively charged holes which move in the direction of I. When a magnetic field B is applied in a direction perpendicular to the direction of current flow, a force $F = (qv \times B)$ causes the carriers to move in a direction which is mutually perpendicular to both the direction of I and to the direction of the B field. This causes a net excess of carriers, both electrons and holes to occur at the lower set of contacts (6,7,8). Consequently, an electric field, called the Hall field (Ref. 20), is realized between the lower (6,7,8) and the upper (2,3,4) sets of contacts. Under steady-state conditions with no net current flow between contacts (3) and (7) the Hall field force will exactly balance the Lorentz

force. If a majority of the carriers displaced to contact (7) are electrons, this contact will show a negative V_H with respect to contact (3) and the sample will be n-type. On the other hand, an excess of holes at (7) will result in a positive V_H with respect to (3) and the semiconductor will be p-type.

2. Calculation of the Hall Coefficient and Conductivity

A quantity called the Hall coefficient R_H has been defined (Refs. 20, 21) as

$$R_H = \frac{V_H \times d}{B \times I} \ (cm^3/coul) \qquad (4)$$

where V_H in mV is measured across the sample as described above, d is the thickness of the thin film in microns, B is the magnetic induction in Wb/m^2, and I is the sample current in mA. Further, the conductivity σ of the sample is

$$\sigma = \frac{I \times \ell}{V_\sigma \times w \times d} \ (1/\Omega\text{-cm}) \qquad (5)$$

where ℓ is the linear distance between two of the contacts which are parallel to the direction of I, in cm (contacts (2) and (4) for example), V_σ is the conductivity voltage in mV measured across these contacts as a result of I, and w is the width of the sample in cm. In the samples used the ratio ℓ/w was equal to 26,900 (Ref. 17). Equation (5) then becomes

$$\sigma = \frac{26900 \times I}{V_\sigma \times d} \ (1/\Omega\text{-cm}) \qquad (6)$$

3. Calculation of the Carrier Concentration and Hall Mobility

If the carrier concentrations are either strongly n-type or strongly p-type the following relations can be used to calculate n(p) and $\mu_e(\mu_n)$.

$$\begin{matrix} n(T) \\ p(T) \end{matrix} = \frac{1}{q \times R_H(T)} \quad (1/cm^3) \tag{7}$$

$$\begin{matrix} \mu_e(T) \\ \mu_n(t) \end{matrix} = R_H(T) \times \sigma(T) \quad (cm^2/V\text{-}sec) \tag{8}$$

where the sign of R_H indicates the carrier type and q is the electronic charge.

4. Evaluation of Near-Intrinsic Samples

In certain cases the sign of R_H changed from a positive value at low temperature ranges to a negative value at higher temperatures. This can be attributed to the following two causes. First, the reversal can be caused by sample inhomogenity, suggesting insufficient annealing time which resulted in both n and p regions in the same sample. Second, it could be caused by a p-type sample whose hole concentration is close to the electron concentration. This is by far the more interesting case. In such cases where both holes and electrons contribute significantly to the electrical properties the Hall coefficient can be written as (Ref. 20)

$$R_H = \frac{r \times (p-b^2n)}{q \times (p+bn)^2} \quad (cm^3/coul) \tag{9}$$

$$b \equiv \frac{\mu_e}{\mu_h} \tag{10}$$

$$r \equiv \frac{\langle \tau^2 \rangle}{\langle \tau \rangle^2} \tag{11}$$

where b is the mobility ratio and τ is the relaxation time, where it is assumed that the relaxation time is the same for electrons and holes. Since μ_e is generally larger than μ_h, $b \geq 1.0$. From equation (9) it can be seen that for a slightly p-type sample, ($p > n$), it is possible for b which is a function of temperature to become large enough such that

$$b^2 n \geq p$$

R_H will then become negative. In n-type samples this reversal will never occur because the numerator of equation (9) will always be a negative quantity.

Since in a near-intrinsic sample the transport properties depend strongly upon both majority and minority carriers, the previously described method of determining $\mu_e(\mu_h)$ and $n(p)$ cannot be used. Using a method described by Tao and others (Ref. 19) the following quantities can be calculated:

1) The electron and hole mobilities μ_e and μ_h.
2) The electron and hole carrier concentrations n and p.
3) The intrinsic carrier concentration n_i.
4) The density of states effective mass m_d^*.

A computer program written by Wang (Ref. 17) was used to solve for these parameters and is included in this report. Table V lists the results of calculations performed on one sample which exhibited Hall reversal characteristics.

5. Equipment Configuration

Electrical measurements were performed on the

TABLE V
INTRINSIC CARRIER CONCENTRATION AND THE DENSITY OF STATES EFFECTIVE MASS AT THF HALL REVERSAL TEMPERATURE FOR SAMPLE SS-10-OB-11-3

Sample Number	T_o °K	n_i (1/cm^3)	M_d^*
SS-10-OB-11-3	287	3.27×10^{16}	.152

$Pd_{0.9}Sn_{0.1}Se$ samples using the equipment shown in Figures 13 and 14. The sample was mounted on one side of a copper cold finger using thermal heat-sink grease. A copper-constantan thermocouple was mounted on a blank substrate on the opposite side. Figure 15 shows a sample mounted on the dewar cold-finger. The thermocouple was connected to the x-axis amplifier of an Omnigraphic Model RR-97 chart recorder. Electrical connections were made to the sample using the copper leads which were attached as described in Section III. A multi-pin vacuum feed-through connected the internal wiring to the measuring equipment. The cold finger and liquid nitrogen reservoir was inserted into the outer dewar assembly which was fastened between the pole pieces of an Alpha Model 6000 6-inch fixed gap electromagnet with a Trygon Model M7C40-500V power supply. The magnet had previously been calibrated to provide a magnetic field strength of 5000 gauss at a field current of 31.5 amperes. The lower portion of the dewar was externally wound with a heating element which allowed faster heating of the sample when desired. A

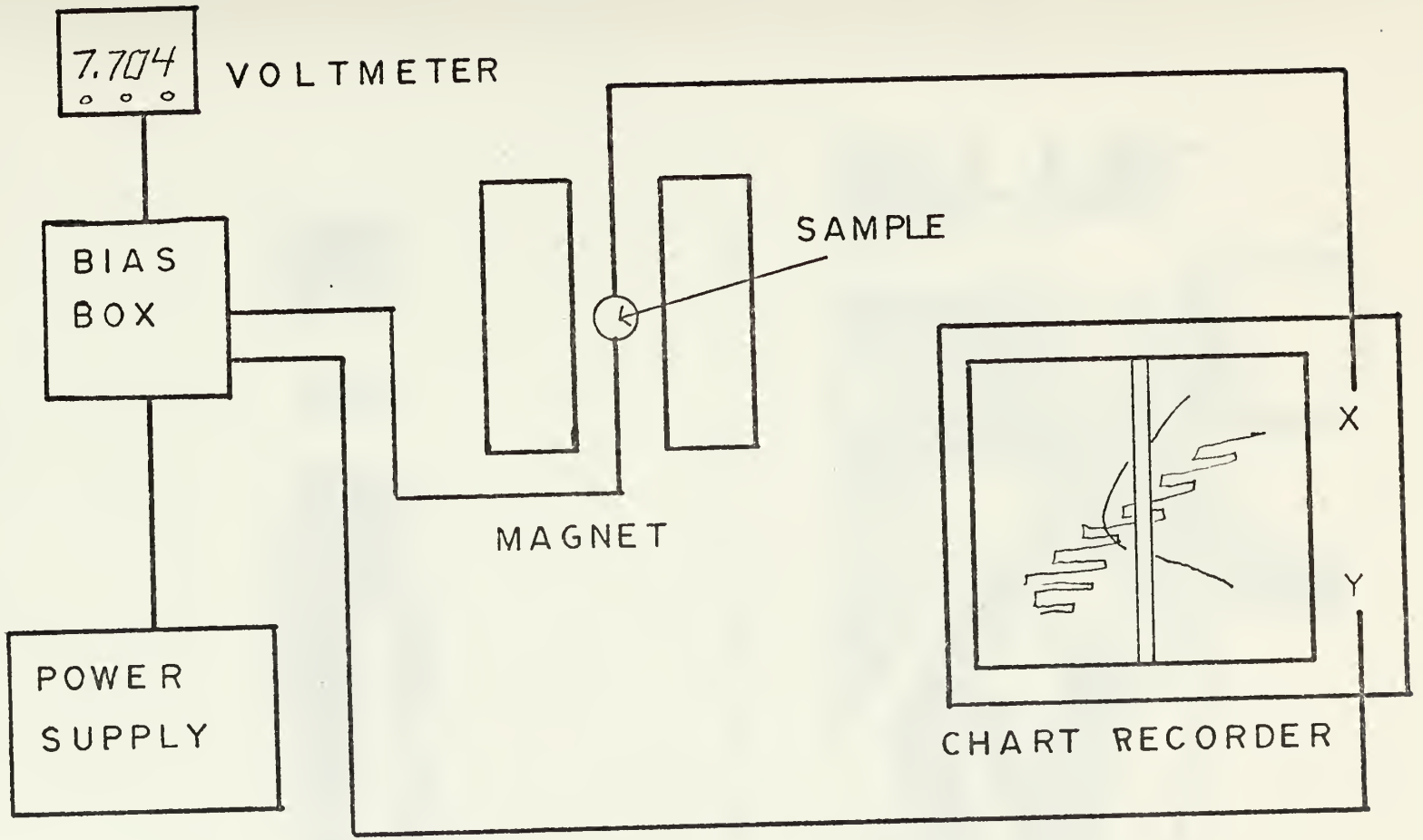

HALL MEASUREMENT EQUIPMENT

Figure 13.

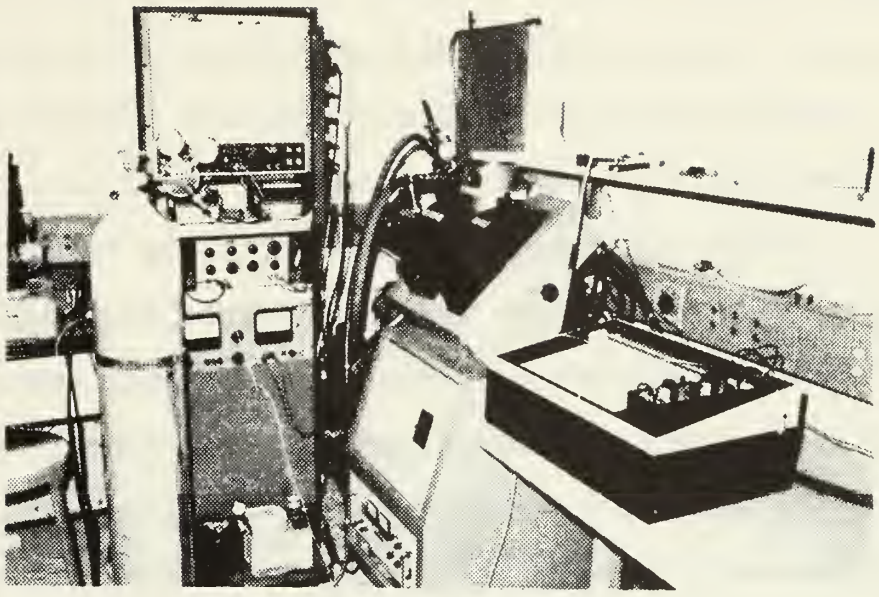

Figure 14. Hall Measurement Equipment.

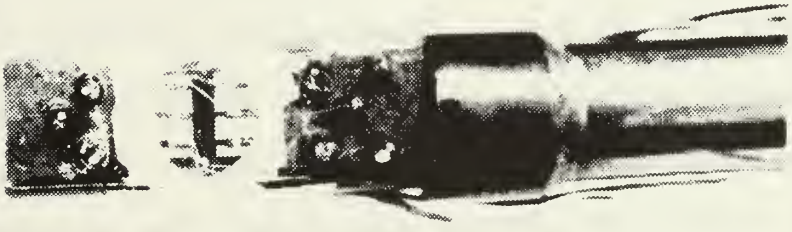

Figure 15. Sample Mounted on Dewar Cold Finger.

Universal Electronics Model 520A laboratory power supply and control box provided a constant current to the sample. In all measurements this current was regulated at one milliamp. The control box was configured to allow voltage readings to be taken off the various serial and parallel combinations of the six contactsarms on the sample, a feature which was often used when one of the sets of contracts became inoperative either due to large contact resistance or due to the breaking of contacts at low temperatures. Additionally, the control box provided for constant dc voltage offsets which were often needed in recording the low temperature Hall voltage excursions.

6. Electrical Measurement Procedures

Once the sample had been mounted on the cold finger it was inserted into the dewar assembly and the system was pumped down with a mechanical vacuum pump to a pressure below thirty microns. Approximately one-half hour prior to making the measurements the filament supply of the current power supply was turned on in order to allow the current to stabilize. The cold finger temperature was measured with a mercury thermometer and the x-axis gain of the chart recorder amplifier was calibrated to this temperature. When the current supply had stabilized sufficiently the bias current through the sample was adjusted to one milliamp. Next, the conductivity voltage between two selected arms on the same side of the sample was measured using a digital multimeter. It was also fed to the y-axis amplifier on the chart recorder.

The y-axis amplifier was calibrated to this voltage and the attenuator set to a value which would allow tracking of the expected voltage range. Once the recording instruments were calibrated, the dewar was cooled to 90°K by adding liquid nitrogen to the reservoir, and the V_σ measurement was made during the cool down. When the temperature had reached its lowest value, the control box was changed to measure the Hall voltage. The sensitivity of the y-axis amplifier was increased to measure the smaller variations in V_H. The sample temperature was then raised to 300°K by purging the reservoir with pressurized air and by applying external heat to the dewar using the heating element. As the temperature was raised, the magnetic field was manually switched on and off and a plot was recorded of V_H vs T. The direction which the recorder pen moved on application of the field can be used to indicate whether the sample was n or p type. The various parameters needed in the computation of μ_e, μ_h n, p, n_i, nad m_d^* were taken directly off of these two plots. Some of the samples exhibited 90°K mobilities on the order of 20-200 cm^2/volt-sec. Their resistances became comparable to the input impedance of the chart recorder amplifiers. It was then necessary to obtain the voltage data using a digital voltmeter. The effects of this loading are shown in Table VI and are further discussed in Section V.

C. PHOTOCONDUCTIVE MEASUREMENTS

Standard photoconductive detector measurements were made on fifteen of the samples. They were chosen to include films

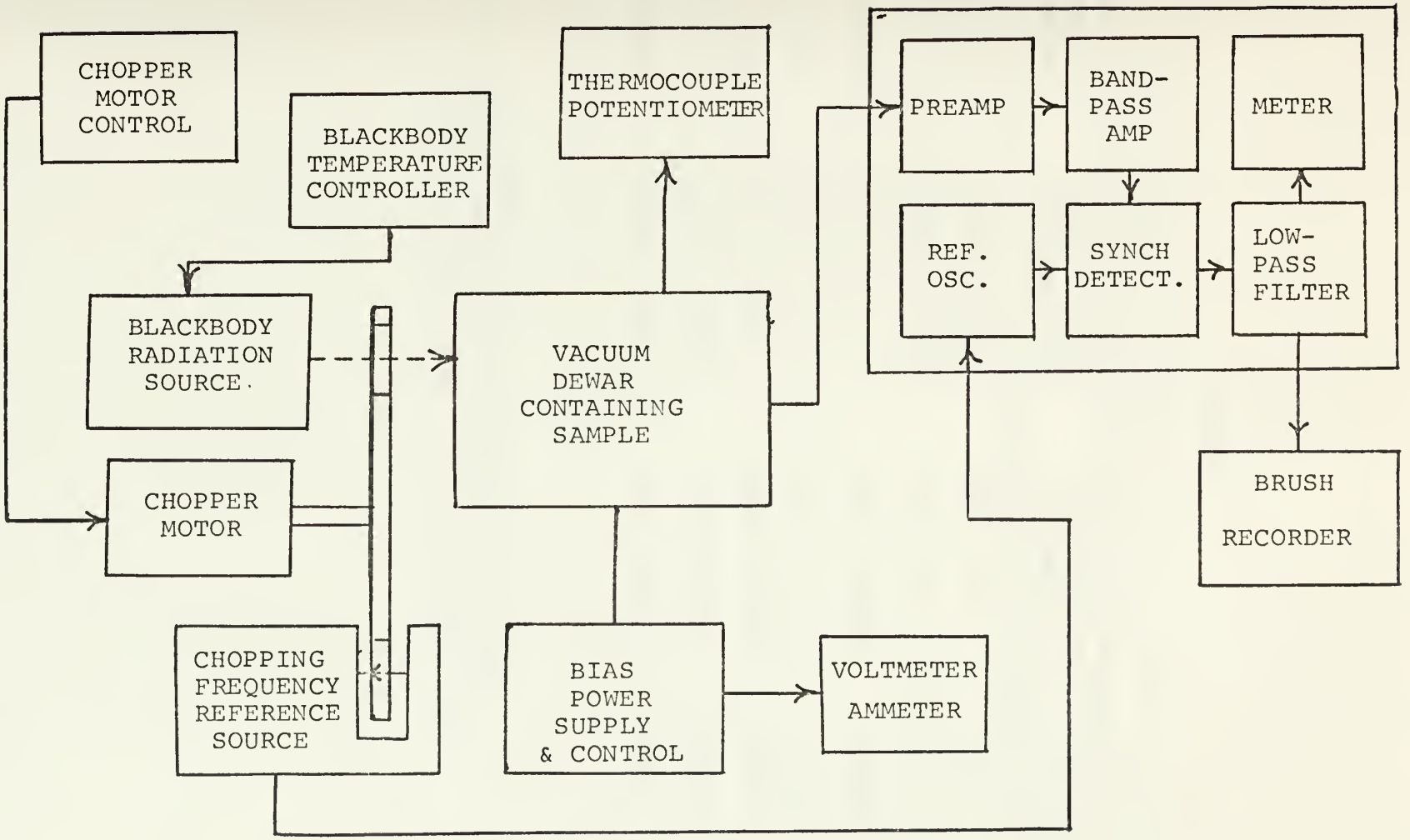

Figure 16. Photoconductive Measurement Schematic.

TABLE VI

LOADING EFFECTS OF CHART RECORDER ON HALL PARAMETERS

Sample Number	Conductivity Voltage (mV)	Hall Voltage (mV)	90°K Mobility (cm^2/V-sec)
OB-11-2	12800 / 1506	30 / 33	139 / 1175
OB-11-3	12000 / 1760	33 / 30	134 / 920
OB-12-4	132 / 90	14.6 / 14.8	5950 / 8978
OB-12-5	26.9 / 60	14.5 / 6.5	29200 / 5828
OB-13-3	620 / 2.42	10.6 / 10.3	920 / 238
OB-13-4	17140 / 5980	8.8 / 9.2	27.7 / 82.5
OB-13-5	4160 / 3940	9.5 / 9.25	123 / 126

Note: The number to the left of the "/" is the unloaded value. That to the right is the loaded value. i.e. No-Load / Load

on BaF_2 and CaF_2 substrates, both single and polycrystal structures with (100), (111), and (100)+(111) mixed orientations, and represented wide range of mobilities and carrier concentrations. Table VII summarizes the results of the photoconductive measurements.

1. Measurement Procedure

Standard 500°K blackbody response measurements were made on the samples according to well established procedures (Refs. 22, 23). Holmquist's thesis (Ref. 14) gives a detailed description of the measurement apparatus, procedures, and results concerned with the samples studied in the research. Additional measurements on the spectral response of sample OB-10-4 and on the photoconductive transient response of samples OB-10-4 and OB-12-3 are also included in this Ref. Figure 16 shows the equipment used in the measurement of the blackbody response.

500°K blackbody radiation from a Barnes Model 11-10T1-1 Blackbody Simulator and temperature controller was chopped by a mechanical chopper, which was maintained at a constant speed by an Electrocraft Model E-550M motor speed controller. All measurements in this report were made at a chopping frequency of 1000 hz. The chopper also provided a 1000 hz signal used as a reference for the lock-in amplifier. The sample was mounted on the cold-finger of a vacuum dewar which incorporated a KRS-5 window. Microdot mini-noise shielded cables were used for all internal and external connections. When the dewar vacuum was less than 20 μ, a sample temperature

TABLE VII

SUMMARY OF PHOTOCONDUCTIVE PERFORMANCE OF $Pb_{0.9}Sn_{0.1}Se$ SAMPLES

Sample Number	Crystal Structure	Carrier Concentration ($1/cm^3$)	Hall Mobility ($cm^2/V\text{-}sec$)	Resistance 300 K/100 K (kohm)	Detectivity ($cm/Hz^{\frac{1}{2}}W$)	Responsivity (V/W)
OB-7-3	PC(100+111)	1.48×10^{17}(p)	1040	.70/.76	7.1×10^{5}	0.45
OB-7-4	PC(100+111)	1.30×10^{17}(p)	4230	.66/.27	2.3×10^{5}	0.034
OB-8-3	PC(100+111)	7.82×10^{16}(p)	6210	.68/.20	2.3×10^{5}	0.045
OB-8-4	PC(100+111)	6.43×10^{16}(p)	7350	.72/.25	1.0×10^{6}	0.11
OB-10-2	SC(100)	5.66×10^{17}(p)	77.0	.9/8.2	2.0×10^{6}	3.8
OB-10-3	SC(100)	1.06×10^{17}(p)	468	2.6/6.4	1.1×10^{7}	18.0
OB-10-4	SC(100)	1.11×10^{17}(p)	504	4.0/9.8	7.2×10^{6}	61.0
OB-11-2	SC(100)	4.90×10^{16}(p)	139	1.7/20.5	7.9×10^{6}	23.0
OB-11-3	SC(100)	5.14×10^{16}(p)	134	1.6/16.0	4.0×10^{6}	23.0
OB-11-5	SC(100)	4.73×10^{17}(p)	1600	.32/.13	6.9×10^{5}	0.09
OB-12-3	SC(111)	5.42×10^{17}(p)	857	1.3/.36	4.9×10^{6}	0.65
OB-12-5	SC(111)	2.29×10^{17}(p)	29200	1.0/.2	1.2×10^{5}	0.035

TABLE VII (Continued)

Sample Number	Crystal Structure	Carrier Concentration ($1/cm^3$)	Hall Mobility ($cm^2/V\text{-}sec$)	Resistance 300 K/100K (kohm)	Detectivity ($cm/Hz^{\frac{1}{2}}W$)	Responsivity (V/W)
OB-13-2	PC(100+111)	1.56×10^{18}(p)	22.0	8.0/12.5	3.1×10^{5}	2.5
OB-13-4	PC(100+111)	3.75×10^{17}(p)	27.7	7.5/17.0	1.3×10^{6}	5.8
K-5-3	PC(100+111)	4.83×10^{17}(p)	1450	.300/.106	7.8×10^{4}	0.003

of approximately 100°K could be maintained. This temperature was measured with a copper-constantan thermocouple which was mounted on a blank CaF_2 substrate in the vicinity of the sample.

The bias current to the sample was provided by a laboratory power supply capable of 500 V dc. A low-noise load resistor for the sample was located in the dewar, and the signal voltage was decoupled by microdot cables. Low-noise mylar capacitors were used to decouple the signal, and also to reduce power supply noise and transients. Bias currents in the range of .5 to 20 mA were used, depending upon the low-temperature sample resistance. Table VII lists both the 300 and 100°K resistance of the samples. A PAR Model 124 Lock-In amplifier was used to measure both the noise and signal voltages. Noise voltages were normalized to a 1 hz bandwidth. Signal voltages were measured using the PAR as a synchronous detector with the 1000 hz reference signal generated at the chopper. Type 118 and type 116 preamplifiers were used for low resistance and high resistance samples, respectively. Sample noise can be determined from the measured noise by using the amplifier noise figures for both preamplifiers supplied by PAR. The signal to normalized noise ratio was measured for each sample at several different bias currents. Detector measurements were made at the optimum bias for the best signal to noise ratio. Detector evaluation was carried out using the standard formulas (Ref. 22).

V. RESULTS AND DISCUSSION

A. METALLURGICAL PROPERTIES

The metallurgical properties of the $Pb_{1-y}Sn_ySe$ thin-films are affected by the substrate type, substrate temperature, and the deposition rate (a function of boat temperature, geometry, and the deposition time). In considering the results obtained on films deposited both for this research and for other uses, the following results are noted.

On BaF_2 substrates, (111) components were present in all depositions. At lower substrate temperatures ($\leq$ 270°C) some (100) structure was observed, however, when the substrate temperature was raised to approximately 300°C, only (111) components existed. This is probably due to the tendency of the film to orient itself along the (111) orientation of the substrate when the vapor ions have enough mobility as they arrive at the substrate surface. This occurs to a greater degree as the temperature of the substrate is raised. This tendency is balanced by the characteristic of the film to grow naturally on (100) planes. The outcome of these two tendencies seems to depend on three factors: the lattice match between the substrate and the crystal, the substrate temperature, and the film growth rate. The lattice parameters of interest are given as (Ref. 17):

	BaF_2	CaF_2	$Pb_{0.8}Sn_{0.2}Se$
Lattice Parameter a (Å)	6.2	5.46	6.11

Because of the closer match between the film and the BaF_2 substrate, it is easier for the film to grow on the (111) planes. This is not the case with CaF_2 substrates. Here the lattice mismatch is larger. At lower substrate temperatures (≃ 285°C) and at deposition rates of about 650 Å/min the films tend to grow on their natural (100) planes and SC(100)[2] films resulted. If the substrate temperature is raised to about 300°C or higher, PC(100)+(111) films resulted. In order to achieve SC(100) films on CaF_2 at higher substrate temperatures, it is necessary to increase the deposition rate to approximately 1000 Å/min. This has the effect of "Freezing" the (100) structure and not allowing the ions to orient themselves with the (111) substrate planes. At still higher substrate temperatures (≃ 375°C), SC(111) on CaF_2 is obtained. The following observations are consistent with the data presented in this report.

1. BaF_2 favors (111) growth; CaF_2 favors (100) growth.
2. Lower substrate temperatures have a tendency to produce (100) orientations. Higher substrate temperatures produce (111) growth.
3. On BaF_2 substrates the better lattice matching

---

[2]SC is single crystal, PC is polycrystalline

(111) growth. No SC(100) growth has been observed on BaF_2.

4. On CaF_2 substrates, SC(100), PC(100)+(111), and SC(111) films can be obtained, depending upon the growth rate and the substratures.

B. ELECTRICAL PROPERTIES

The 90°K carrier concentration and mobility were measured on all samples after isothermal annealing at temperatures between 300 and 325°C. The following trends were noted.

Mobilities varied between 10 and 29000 cm^2/V-sec. SC(111) films showed generally higher mobilities than SC(100) films. PC(100)+(111) films on Caf_2 showed the greatest variation in mobilities. It appears that the amount of (111) structure present in these PC samples has a large effect on their mobilities. The PC(111)+(100) film on BaF_2 which was annealed at 319.5°C (K5-4) had mobilities similar to PC(100)+(111) films on CaF_2 annealed at 310.5°C. As is noted in Table IV, poor regulation of the annealing ovens caused some samples to reach temperatures higher than the listed annealing temperature. It is likely that some of the inconsistent electrical and photoconductive effects were caused by inhomogeneous samples, or by samples whose annealing cycle had created junctions in the samples. Carrier concentrations varied with deviations from stochiometry as stated in Ref. 16. Figure 9 shows the variations in carrier concentration with annealing temperature. Based upon the results of this research, the lower stochiometric annealing

temperature for $Pb_{0.9}Sn_{0.1}Se$ was determined to be approximately 319.5°C. Temperatures above 319.75°C were consistently n-type and those below 319.5°C were p-type. Some exceptions existed and fall into two categories. First, regulation of the annealing ovens permitted temperatures to deviate from the nominal annealing temperature. Some of these deviations were considerable, and the length of time which the samples were exposed to these elevated temperatures is in most cases unknown. These conditions could result in a sample being annealed at a temperature considerably higher than that which was recorded. Second, in a few cases, both of the samples within one annealing ampoule were not equally exposed to the metal-rich vapor due to one sample overlapping the other. This could result in one sample being n-type and the other p-type. P-type samples above 319.5°C and all n-type samples below this temperature (one in each case) fall into these two categories. Results obtained during Hall measurements further showed tendencies of low-temperature Hall coefficient reversal indicating sample inhomogeneity in those samples annealed with questionable temperature regulation. On the other hand, several of the samples either had high-temperature reversals of R_H or showed tendencies toward a reversal at temperatures higher than 300°K. These samples also support the estimate of the stochiometric temperature where the samples became well compensated or near-intrinsic. Figures 17-22 are plots of R_H vs 1000/T and σ vs 1000/T obtained from electrical measurements on selected samples.

It is important to note that for some of the high resistance samples the values plotted on a chart recorder are not accurate due to loading when the resistance of the sample becomes comparable to the input impedance of the chart recorder. In these cases, the values of V_H and V_σ were measured on a digital voltmeter with the chart recorder disconnected. Often, the values obtained in this manner were very different from those obtained on the recorder. Table VI shows the effects of this loading on certain samples. Figure 23 is a diagram of the carrier concentration vs mobility. All n-type samples measured had carrier concentrations between 3 and 5.4×10^{17} $1/cm^3$.

C. PHOTOCONDUCTIVE RESULTS

500°K blackbody signal voltages in the range from .21 to 1300 μV were measured. Normalized noise voltages varied from .02 to 3.8 μV. The responsivities and detectivities for all samples are listed in Table VII. The highest response was generally measured for samples which were SC(100) and had low mobilities. SC(100) crystals with higher mobility (OB-11-5) had lower responsivity. Films containing (111) and (111)+(100) orientations usually exhibited low responsivities. Samples OB-13-2 and OB-13-4 were two exceptions which had PC(100)+(111) structure, but relatively good responsivities. It is discussed in Holmquist's thesis that this could have been caused by the high degree of (100) component compared to a small degree of (111) component found in these samples. The Laue photograph indicates a high degree

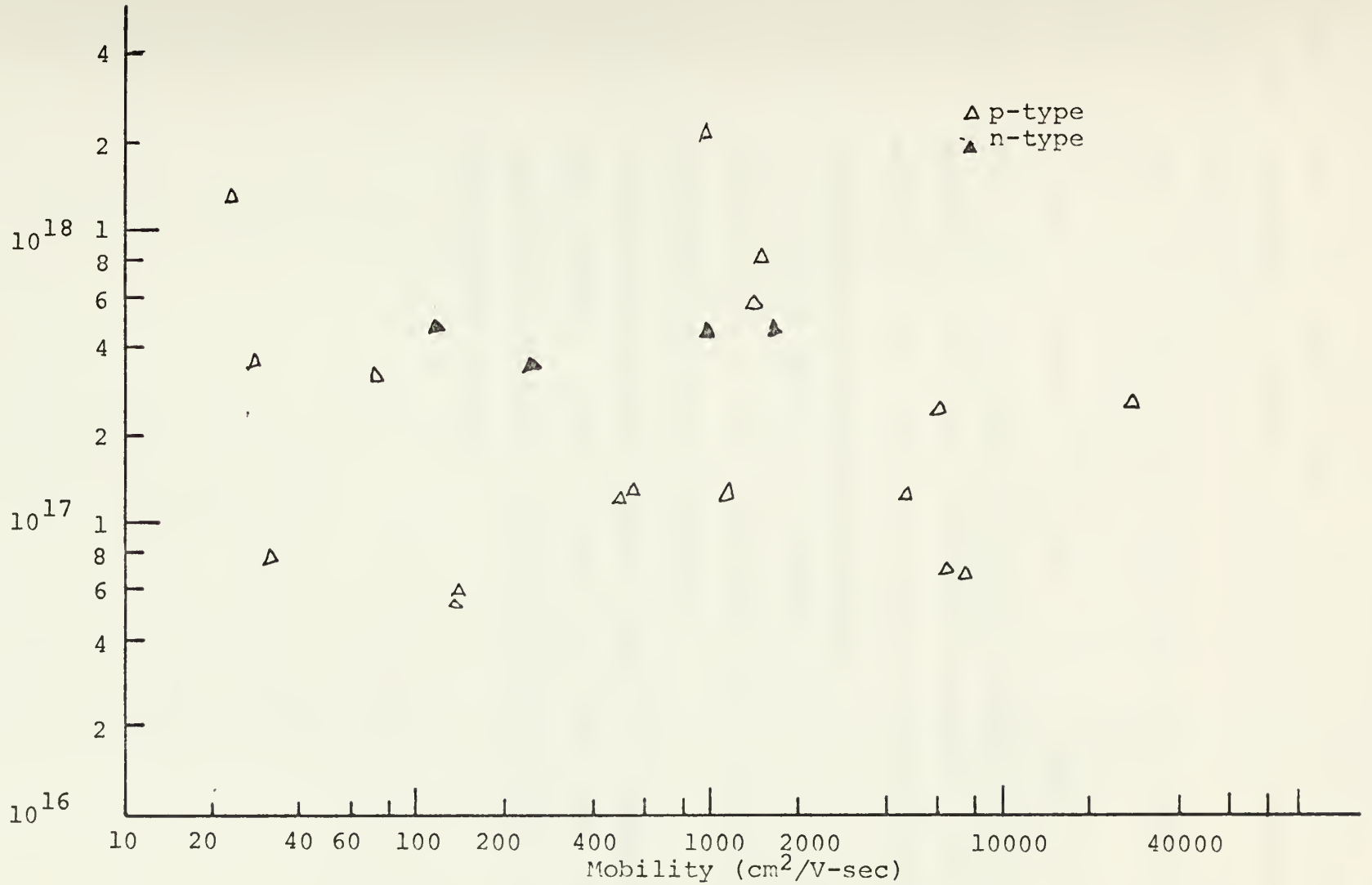

Figure 23. Variation of Carrier Concentration with Mobility at 90°K.

of single crystal structure, while the diffractometer scan showed strong (100) family lines and weak (111) family lines.

The following conclusions are made based upon examination of the available data.

1. (100) films have better photoconductive response than both PC(100)+(111) and SC(111) films.
2. In those films which do have a (111) component, the ones with lower measured values of mobility have generally better photoconductive response. This is valid only when comparing films of the same deposition batch and crystal structure.
3. Well matched crystal structures, i.e. (111) single-crystal film on (111) substrates does not suggest good photoconductive response.
4. The low detectivities are the result of excessive noise, mostly of the 1/f type, and most likely the result of rectifying junctions caused by the silver-epoxy bonding method.

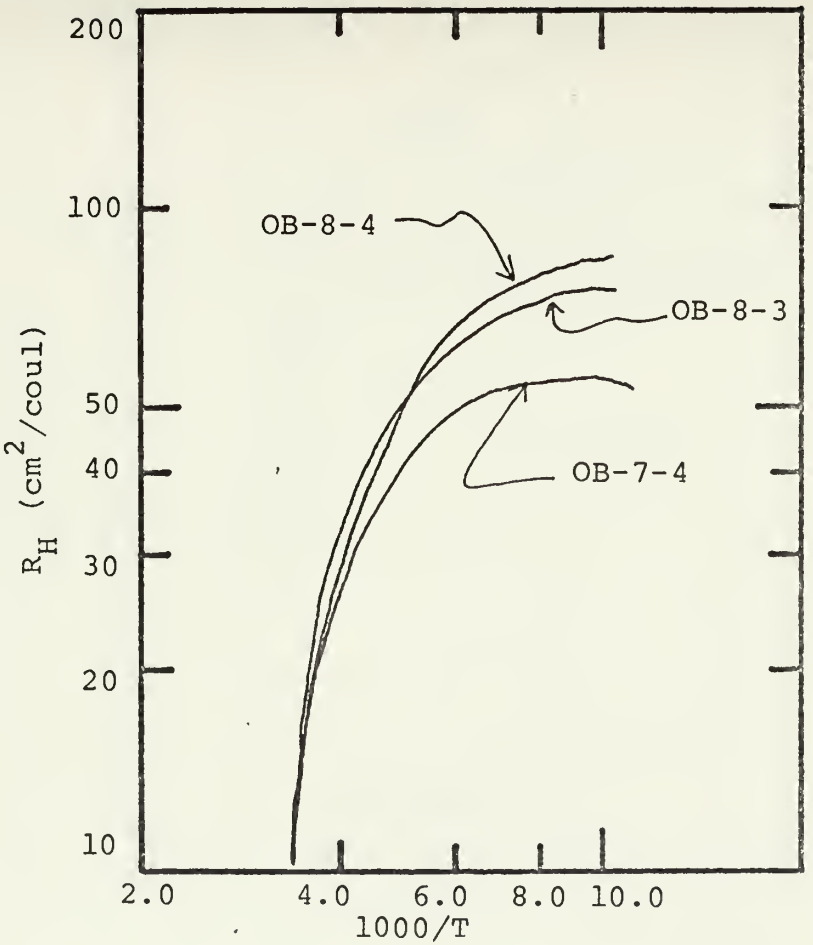

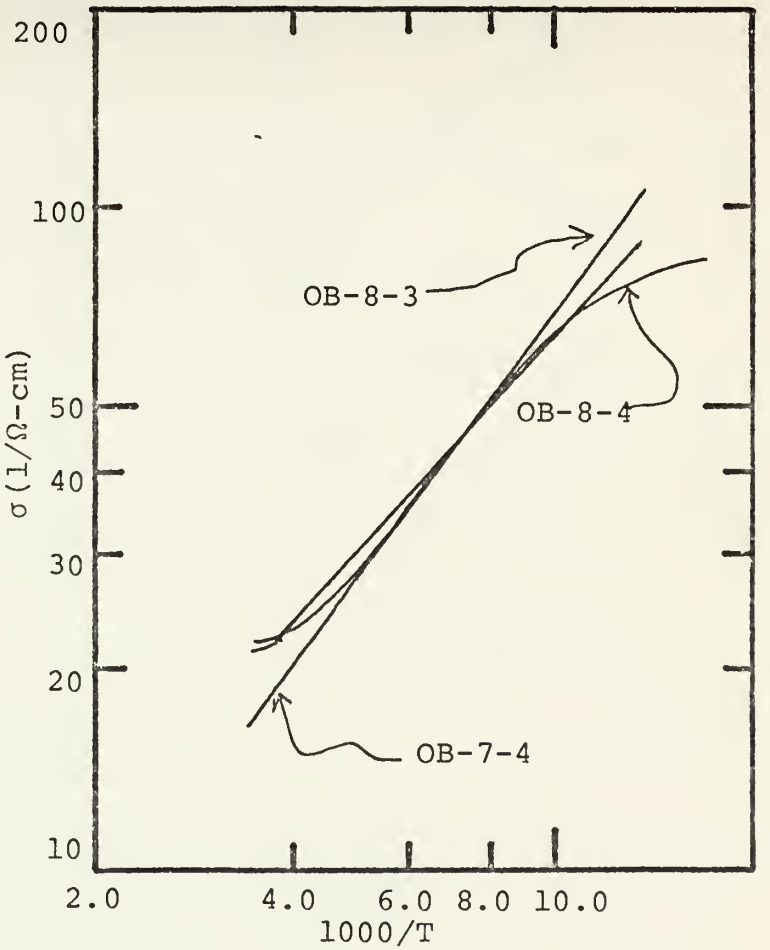

Figure 17. Temperature Variation of R_H and for Samples SS-10-OB-7-4.
-8-3
-8-4

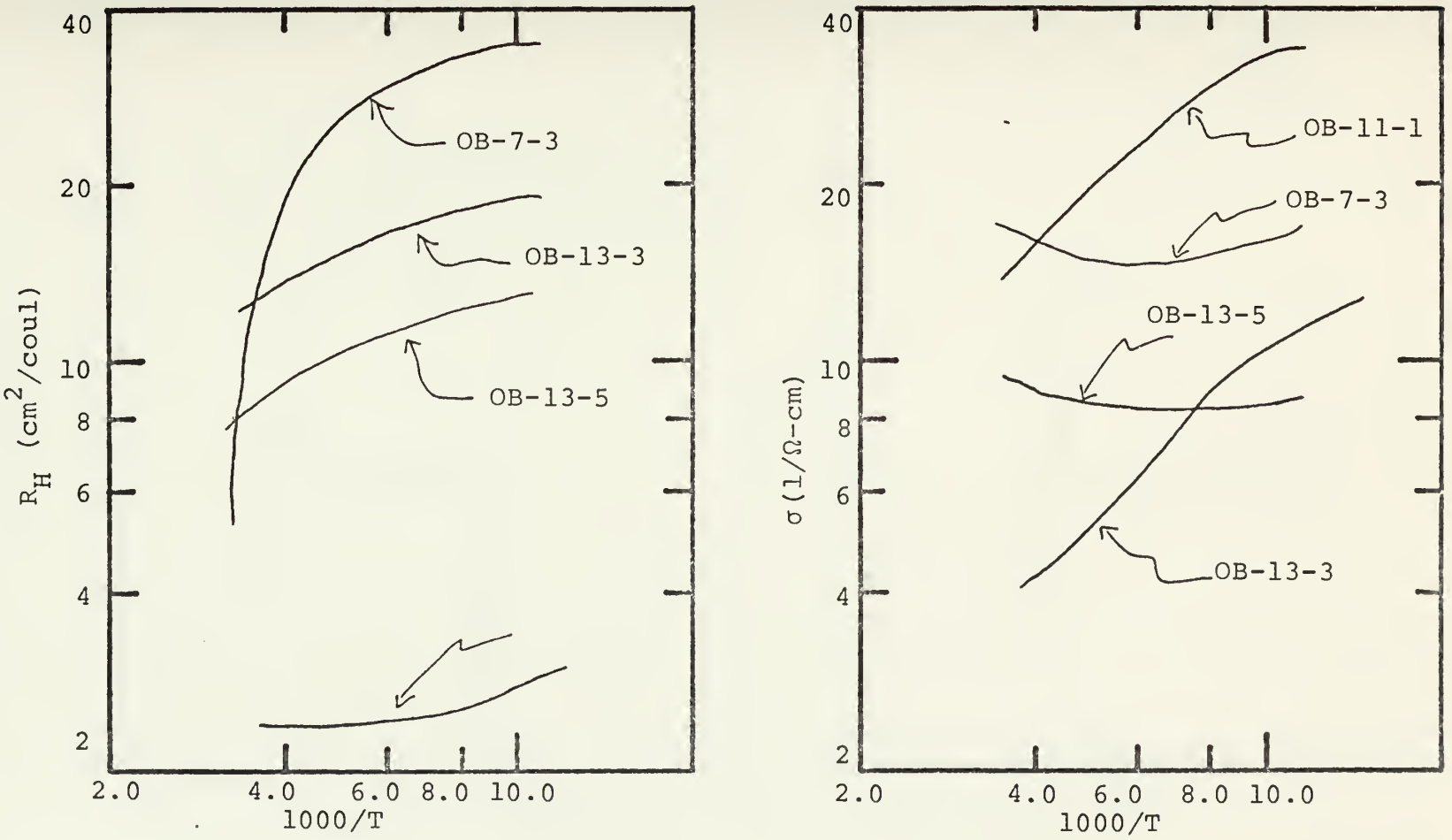

Figure 18. Temperature Variation of R_H and σ for Samples SS-10-OB-7-3.
-13-3
-13-5
-11-1

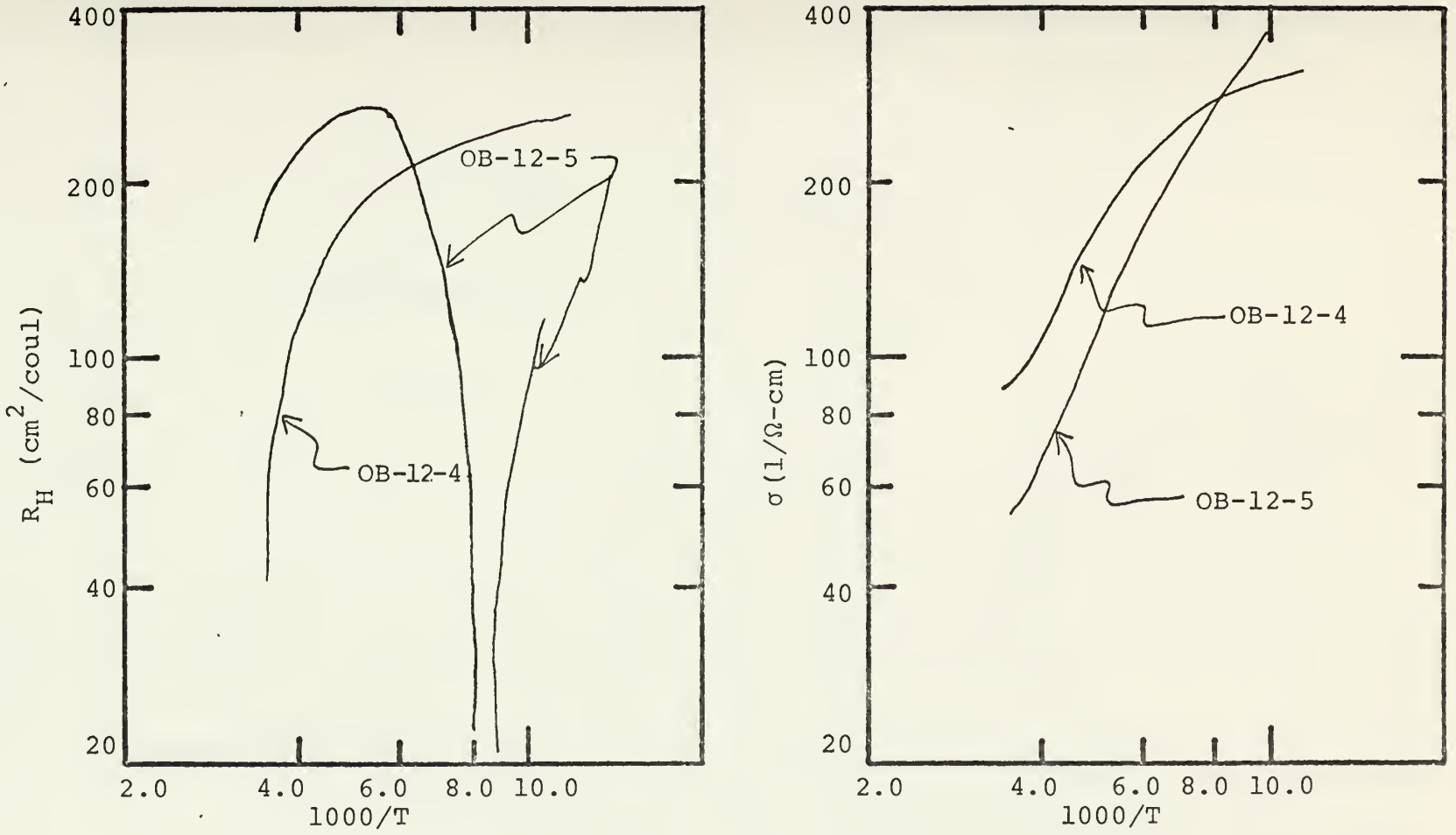

Figure 19. Temperature Variation of R_H and σ for Samples SS-10-OB-12-4. -12-5

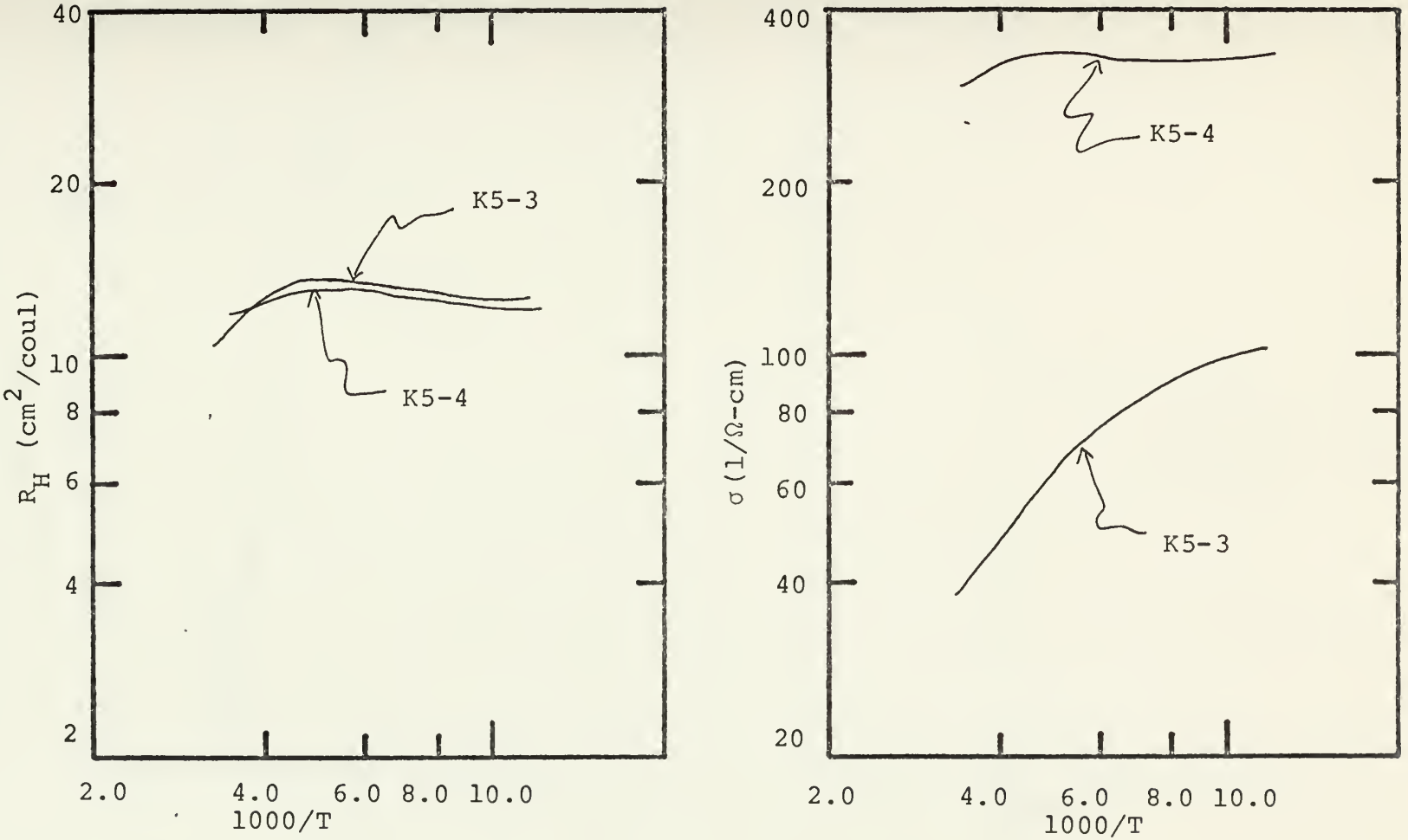

Figure 20. Temperature Variation of R_H and σ for Samples SS-10-K5-3. K5-4

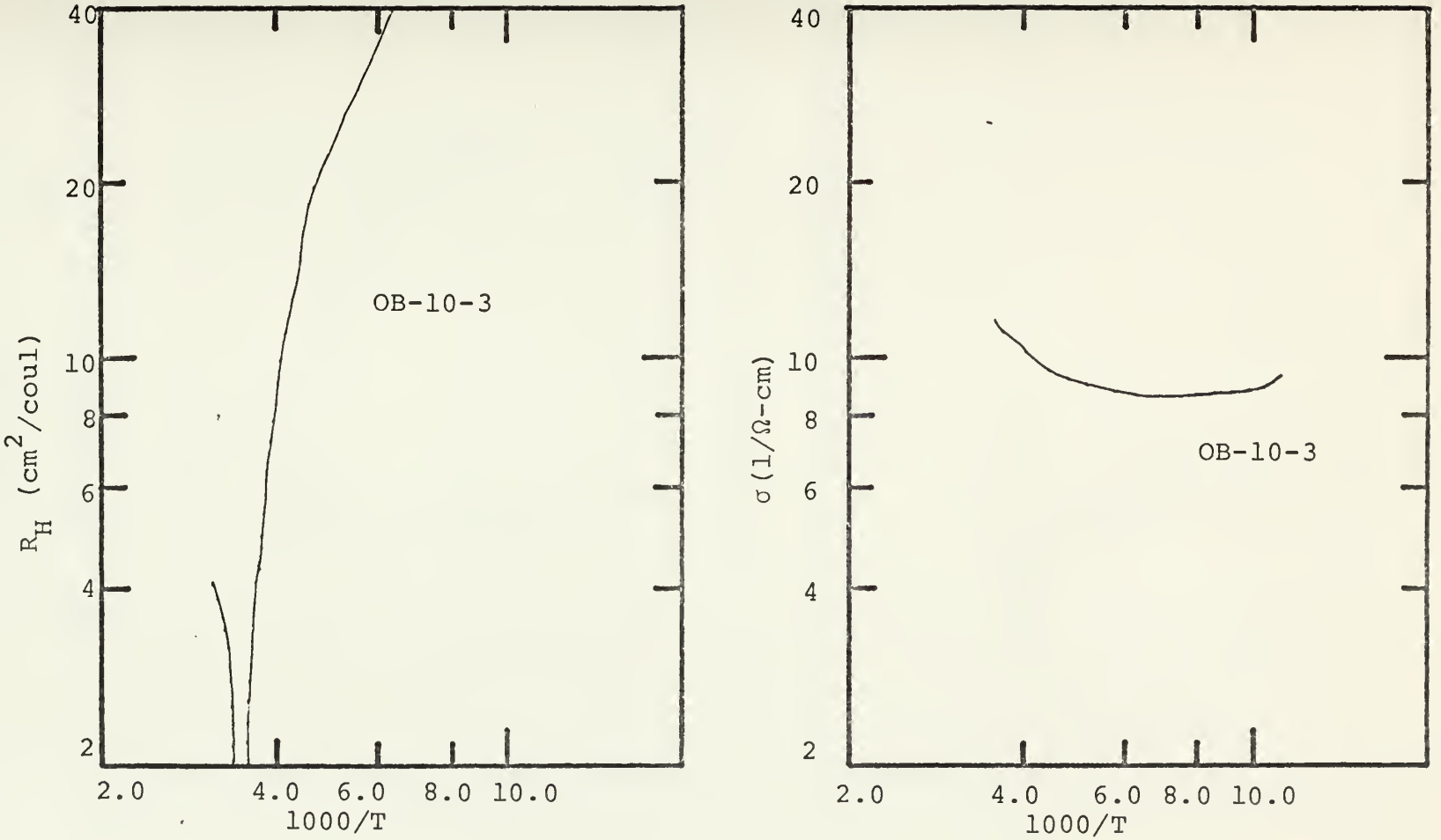

Figure 21. Temperature Variation of R_H and σ for Sample SS-10-OB-10-3.

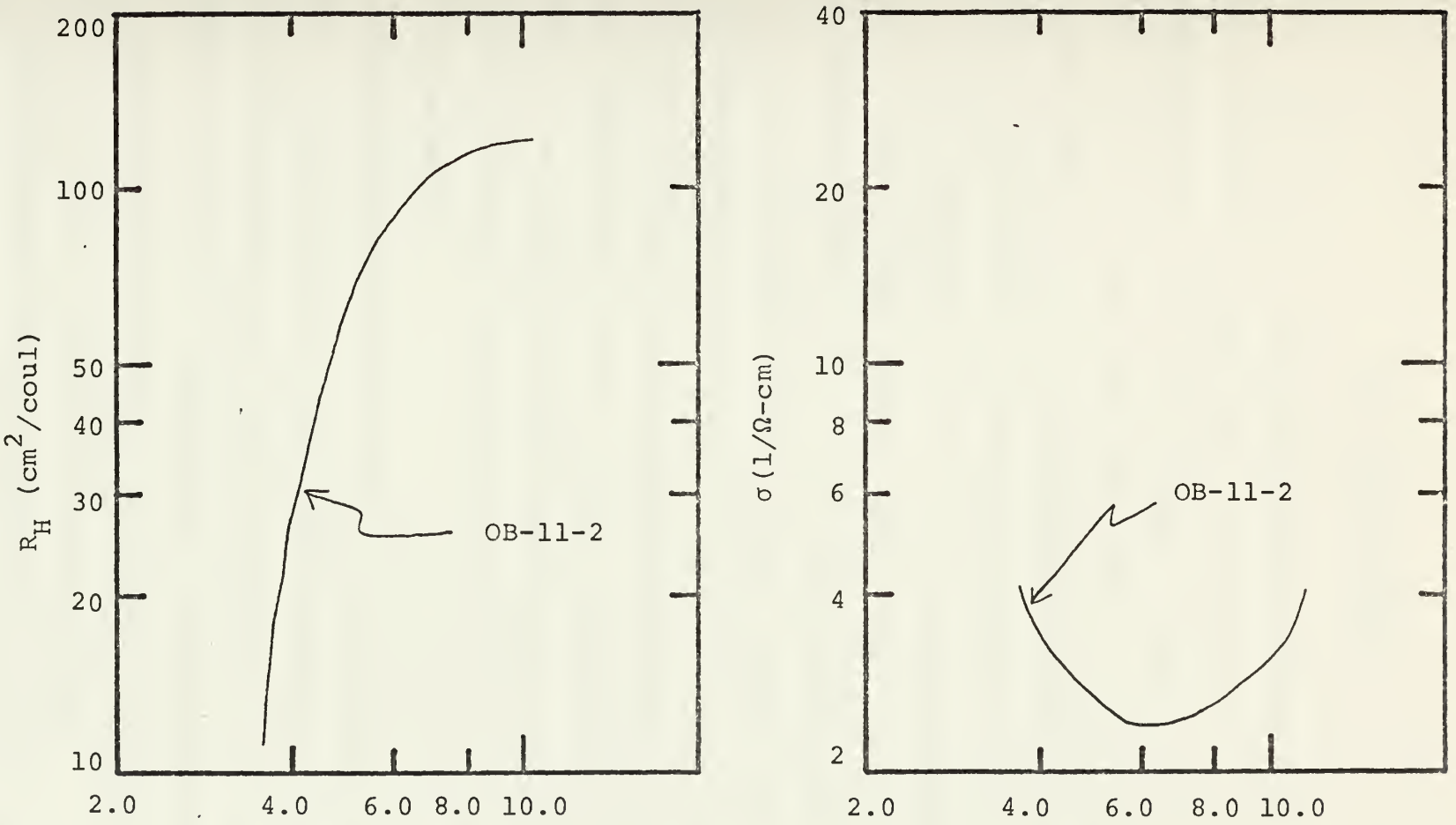

Figure 22. Temperature Variation of R_H and σ for Sample SS-10-OB-11-2.

VI. CONCLUSIONS

The one-boat deposition method produced reproducible thin films of $Pb_{0.9}Sn_{0.1}Se$. By controlling the deposition parameters and substrate material, SC(100), SC(111), and PC(100)+(111) films can be deposited on CaF_2. SC(111) and PC(111)+(100) films can be deposited on BaF_2. It is unlikely that SC(100) films can be attained on BaF_2.

(100) films were observed to have lower mobilities than (111) films. Single crystal (111) on BaF_2 had the highest mobilities and the lowest 100°K sample resistances. These films also had lower responsivities. SC(100) films with low mobilities had the highest responsivities. The amount of (111) component in the crystal films appears to have a significant effect on the mobility, resistance, and photoresponse and generally reduce the mobility and responsivity. PC(100) or PC(111) films were not obtained on either substrate material.

The highest blackbody responsivity obtained was 60 V/W which is approaching the best reported value of 100-125 V/W for photovoltaic $Pb_{1-x}Sn_xTe$ detectors. The bias current needed to achieve this responsivity was approximately 1 mA.

The detectivity, however, was lower than expected and can be improved by reducing the contact noise.

The isothermal annealing resulted in carrier concentrations generally in the mid-10^{16} to mid-10^{17} range. The

lower stochiometric annealing temperature T_1 was determined to be ≈ 319.5°C for $Pb_{0.9}Sn_{0.1}Se$. No study was made correlating the pre and post annealing mobilities.

The carrier concentrations were low enough in some cases that the Hall coefficient changed sign in the temperature range from 300 to 90°K This allowed calculation of the intrinsic carrier concentration and the density of states effective mass. The values obtained on the one sample tested were not in agreement with earlier results obtained in our group. It is believed that some of the accuracies in thin film thickness determination and in the Hall voltage calculation should be improved.

Two areas of this research require improvement. The first concerns the temperature regulation and monitoring of the annealing ovens. It is suggested that high accuracy proportional controllers be used, and that a method of continuously recording the actual sample temperature be employed. This can possible be done using a long-duration strip chart or drum recorder. It would also be possible to modulate a low-speed magnetic tape and then use an A/D converter to record it on a computer. The second area which requires attention is in the measurement of the higher resistance samples which have a tendency to load the chart recorder and give erroneous Hall measurements. This problem could be reduced by using a high impedance recorder and a highly regulated bias current supply. This area is also adaptable to digital processing techniques which could reduce the work

load and increase the accuracy. Investigation should be made into the effects of partial pressures (PV=nRT) within the annealing ampoules, and also on the effects of raising the annealing temperature intentionally for various time periods during the annealing cycle. Additional studies should be made to determine the relationships between the film thickness, helium gas back-fill pressure, metal-rich source surface area, and the time required to reach thermal equilibrium. One last, but extremely important area of improvement is that of contact noise reduction. It is obvious that the silver-epoxy method as employed was not satisfactory for use in fabricating photodetectors. Other methods of bonding the wire leads to the contacts should be explored.

COMPUTER PROGRAM FOR THE DETERMINATION
OF CARRIER CONCENTRATIONS AND
MOBILITIES IN PB SN SE

DATA IS STARTED FROM THE LOWEST TEMPERATURE

D=THICKNESS IN MICRONS
B=MOBILITY RATIO MUN/MUP
BO=MOBILITY RATIO AT HALL REVERSAL TEMPERATURE
BO=VC(EXT)/VC(EXT)-VC(0)
EG=ENERGY GAP IN EV
EGO=ENERGY GAP AT 0 DEGREES KELVIN
T=TEMPERATURE IN DEGREES KELVIN
TO=TEMPERATURE AT HALL REVERSAL IN DEGREES KELVIN
VH=HALL VOLTAGE IN MV
VH IS POSITIVE FOR P-TYPE, NEGATIVE FOR N-TYPE
VC=CONDUCTIVITY VOLTAGE IN MV
XII=NUMBER OF DATA CARDS
PE=P-N
Z=WAVELENGTH IN MICRON

PROGRAM STARTS

```
      DIMENSION VH(30),VC(30),T(30),R(30),T1(30),C(30),Z(30)
     1HH(30)
      XM=9.107E-28
      H=6.625E-27
      XK=1.380E-16
      Q=1.600E-19
    5 READ(5,105,END=999) D,BO,EGO,TO,XII
  105 FORMAT(8F10.2)
      PRINT 101
      IF(D.LE.0.) GO TO 999
      PE=0.
      GAMA=0.0
      IM=XII
   10 READ(5,175)(VH(I),VC(I),T(I),I=1,IM)
  175 FORMAT(3F10.2)
C
C           CALCULATE THE HALL COEFFICIENT AND CONDUCTIVITY
C
C     0.5 IS FOR MAGNETIC FIELD = 0.5 WEBER/M**2
C     26900 IS FOR HALL SAMPLE
C     SAMPLE CURRENT IS 1 MA
C     EG(T)=EG(0)+5.0*10-4*T FOR PB SN SE
  200 DO 300 I=1,IM
      EG(I)=EGO+5.0E-4*T(I)
      Z(I)=6.625*0.3/(1.6*EG(I))
C     0.85 IS A FACTOR TO CORRECT FOR THICKNESS
      R(I)=0.85*VH(I)*2.0*D
      C(I)=26900.0/(VC(I)*0.85*D)
      T1(I)=1000.0/T(I)
      IF (PE.LE.0.) PE=1./(R(I)*Q)
C
C           CALCULATE THE CARRIER CONCENTRATIONS, N, P, NI
C
C     HE=1
C     HH=0.89 AT 90 DEG INCREASING TO 1.0 AT 200 DEG
C     HH=1.0 BEYOND 200 DEG
      HH(I)=1.
      IF(T(I).LT.90.0) T(I)=90.
  300 IF(T(I).LT.200.) HH(I)=0.89+0.001*(T(I)-90.)
   32 PRINT 102,GAMA
      DO 310 I=1,IM
      IF(R(I).EQ.0.) XN=HH(I)*PE/(BO**2-HH(I))
      IF(R(I).EQ.0.) GO TO 30
      B=BO*(T(I)/TO)**GAMA
```

```
      XB2=2*R(I)*Q*PE*(B+1.)+B**2-HH(I)
      AC=4*R(I)*Q*(B+1.)**2*(R(I)*Q*PE*PE-HH(I)*PE)
      AC=XB2**2-AC
      IF(AC.LT.0.) PRINT 110,R(I),C(I),T(I),GAMA,I
      IF(AC.LT.0.) GO TO 310
  110 FORMAT(1HO,40X,'P CAN NOT BE FOUND,R=',F10.2,'  SIGMA=
     1'  T1=',F8.2,'  GAMMA=',F5.1,'  I=',I2)
      AC=SQRT(AC)
      XN=(-XB2+AC)/(2*R(I)*Q*(B+1.)**2)
   30 P=PE+XN
      YN=XN
      XN=ABS(XN)
      XNI=SQRT(XN*P)
C
C           CALCULATE THE MOBILITIES
C
      XMUP=C(I)/(Q*(XN*B+P))
      XMUN=B*XMUP
C
C           CALCULATE THE DENSITY STATE EFFECTIVE MASS
C
      XT=-EG(I)*1.6E-12/(6.*XK*T(I))
      XT=EXP(XT)*SQRT(2.*3.14159*XK*T(I))
      YT=H*(XN*P/4.)**(1./6.)
      YT=YT/XT
      XME=YT**4
      XME=XME/(XM**2)
      YME=SQRT(XME)
      PRINT 120,T(I),T1(I),YME,YN,P,XNI,XMUP,XMUN,Z(I),EG(I)
     1,C(I),B
  120 FORMAT(1X,2F8.2,F8.3,3E12.4,2F10.2,2F8.4,F8.3,3F7.2)
  101 FORMAT(1H1,7X,'T  1000/T',2X,'    M*',11X,'N',11X,'P',
     112X,'NI',7X,'MUP',7X,'MUN  MICRON      EG   ME*MH',5X,
     2'R',2X,'SIGMA',4X,'B'//)
  102 FORMAT(1HO,1X,'GAMMA=',F5.2)
  310 CONTINUE
      GAMA=GAMA-0.25
      IF(GAMA.GE.-3.) GO TO 32
      GO TO 5
  999 PRINT 123
  123 FORMAT(1H1,'FINIS')
      STOP
      END
```

LIST OF REFERENCES

1. Harmon. T. C., and Melngailis, I., "Single Crystal Lead-Tin Chalcogenides," Ch 4 from Semiconductors and Semi-Metals, vol. 5, ed by R. Willardson and A. Beer, Academic Press, 1970.

2. Harmon, T. C., "Narrow Gap Semiconductor Lasers," J. Phys. Chem. Solids., 32, Suppl. 1, p. 363, 1971.

3. Harmon, T. C., and Melngailis, I., Appl. Phys. Ltrs. 13, p. 180, 1968.

4. Air Force Materials Laboratory Report AFML-TR-71-238, Narrow Gap Semiconductors, by T. F. Tao and C. C. Wang, p. 10, 12-13, 35, 67, 137-141, Dec. 1971. (unpublished)

5. Holloway, H., and Logothetis, E., J. Appl. Phys. 43, p. 256, 1972.

6. Strauss, A. J., "Metallurgical and Electronic Properties of Pb-Sn Se, Pb-Sn-Te, and Other IV-VI Alloys," Trans. TMS-AIME, v. 242, p. 354-371, Mar. 1968.

7. Strauss, A. J., "Inversion of Conduction and Valence Bands in Pb-Sn-Se Alloys," Phys. Rev., v. 157, no. 3, p. 608-611, 15 May 1967.

8. Hoff, G. F., Band Inversion and the Electrical Properties of Lead-Tin Selenide Semiconducting Alloys, Ph.D. Thesis, U. of Md., 1970 .

9. The Physics of Semimetals and Narrow Gap Semiconductors, 1st ed., p. 303-437, Pergamon Press, Inc., 1971.

10. Dimmock, J. O., Melngailis, I., and Strauss, A. J., "Band Structure and Laser Action in Pb-Sn-Te," Phys. Rev. Ltrs., v. 16, no. 26, p. 1193-1196, 27 June 1966.

11. Kittel, C., Introduction to Solid State Physics, 3rd. ed., p. 12-36, 253, Wiley, 1967.

12. Calawa, A. R., and others, "Temperature and Compositional Dependence of Laser Emission in Pb-Sn-Se," App. Phys. Ltrs., v. 14, no. 11, p. 333-334, 1 June 1969.

13. United States Army Electronic Command R&D Technical Report No. DAA-K02-69-C-0069, Photoconductive Infrard Detectors Using Thin Films of Lead-Tin Chalcogenide Alloys, 2nd. Annual Report, by T. F. Tao, I. Kasai, and C. C. Wang, Sept. 1971.

14. Holmquist, K., Thin Film $Pb_{0.9}Sn_{0.1}Se$ Infrared Photoconductive Detectors, Part II: Photoconductive Measurements, Master's Thesis, Naval Postgraduate School, Dec. 1o72.

15. Allgaier, R. S., and Brebrick, R. F., "Composition Limits of Stability of PbTe," Jour. Chem. Phys. v. 32, no. 6, p. 1826-1831, June 1960.

16. Calawa, A. R., and others, "Crystal Growth, Annealing and Diffusion of Lead-Tin Chalcogenides," Trans. TMS-AIME, v. 242, p. 371-373, March 1968.

17. Wang, C. C., Properties of Thin Film Lead-Tin Telluride and Lead-Tin Selenide Infrared Photoconductors, Ph.D. Thesis, UCLA, 1971.

18. Krikorian, K. V., Study of Photoconductivity in Lead-Tin Telluride Thin Films, Master's Thesis, UCLA, 1971

19. UCLA Engineering Report No. 7159, Photoconductive Infrared Detectors Using Thin Films of Lead-Tin Chalcogenide Alloys, T. F. Tao, I. Kasai, and C. C. Wang, September 1971

20. Sze, S. M., The Physics of Semiconductor Devices, p. 42-46, Wiley, 1969.

21. Putley, E. J., The Hall Effect and Related Phenomena, p. 23-25, Buttersworth, London, 1960.

22. Hudson, R. D., Jr., Infrared System Engineering, p. 20-60, 305-346, Wiley, 1969.

23. Handbook of Military Infrared Technology, W. L. Wolfe, ed., p. 457-515, 757-780, USGPO, Wash. D.C., 1965.

INITIAL DISTRIBUTION LIST

		No. Copies
1.	Defense Documentation Center Cameron Station Alexandria, Virginia 22314	2
2.	Library, Code 0212 Naval Postgraduate School Monterey, California 93940	2
3.	Assoc. Professor T. F. Tao, Code 52 Department of Electrical Engineering Naval Postgraduate School Monterey, California 93940	5
4.	Dr. R. G. Morris, Code 421 Office of Naval Research Arlington, Virginia	1
5.	Mr. R. Hickmott AFML/LPE Air Force Materials Laboratory Wright Patterson Air Force Base, Ohio 45433	1
6.	LT/jg Kurt Holmquist, USN 7011 Seacliff Rd. McLean, Va. 22101	1
7.	Capt. William G. McBride, Jr. USMC 705 Asilomar Blvd., Apt. #3 Pacific Grove, California 93950	1

UNCLASSIFIED
Security Classification

DOCUMENT CONTROL DATA - R & D

(Security classification of title, body of abstract and indexing annotation must be entered when the overall report is classified)

ORIGINATING ACTIVITY (Corporate author)

Naval Postgraduate School
Monterey, California 93940

2a. REPORT SECURITY CLASSIFICATION

Unclassified

2b. GROUP

REPORT TITLE

THIN FILM $Pb_{0.9}Sn_{0.1}Se$ PHOTOCONDUCTIVE INFRARED DETECTORS, PART I: METALLURGICAL AND ELECTRICAL MEASUREMENTS

DESCRIPTIVE NOTES (Type of report and, inclusive dates)

Master's Thesis; December 1972

AUTHOR(S) (First name, middle initial, last name)

William Godfrey McBride, Jr.; Captain, United States Marine Corps

REPORT DATE	7a. TOTAL NO. OF PAGES	7b. NO. OF REFS
December 1972	89	23

CONTRACT OR GRANT NO.	9a. ORIGINATOR'S REPORT NUMBER(S)
PROJECT NO.	9b. OTHER REPORT NO(S) (Any other numbers that may be assigned this report)

DISTRIBUTION STATEMENT

Approved for public release; distribution unlimited.

SUPPLEMENTARY NOTES	12. SPONSORING MILITARY ACTIVITY
	Naval Postgraduate School Monterey, California 93940

ABSTRACT

$Pb_{0.9}Sn_{0.1}Se$ thin films were deposited onto cleaved (111) CaF_2 and BaF_2 substrates by either an open one-boat evaporation method or a Knudson type graphite boat method. On CaF_2, single crystal (100), (111), and polycrystalline (100)+(111) films were obtained. On BaF_2, single crystal (111) and polycrystalline (111)+(100) films were achieved. As-deposited films were not photosensitive. Photoconductivity was observed after isothermal annealing in Pb/Sn rich vapor to reduce their carrier concentrations to the mid-10^{16} to mid-10^{17} range. (100) films were more sensitive than either single crystal (111) or polycrystalline (100)+(111) films. At 100°K, 500°K blackbody responsivities up to 60V/W have been developed, compared with the best blackbody responsivities around 100-125 V/W reported for commercial photo-voltaic detectors of $Pb_{1-x}Sn_xTe$ operated at 77°K.

DD FORM 1 NOV 65 1473 (PAGE 1)
S/N 0101-807-6811

UNCLASSIFIED
Security Classification

A-31408

KEY WORDS	LINK A		LINK B		LINK C	
	ROLE	WT	ROLE	WT	ROLE	WT
PHOTOCONDUCTORS						
PHOTODETECTORS						
LEAD-TIN SELENIDE						
INFRARED DETECTORS						
THIN-FILM DETECTORS						

Thesis
M1625 McBride
c.1

Thin film $Pb_{0.9}Sn_{0.1}Se$ photoconductive infrared detectors, metallurgical and electrical measurements.

141391

Thesis
M1625 McBride
c.1

Thin film $Pb_{0.9}Sn_{0.1}Se$ photoconductive infrared detectors, metallurgical and electrical measurements.